Response to Referee #1's review on the GMD-D paper of Sutanudjaja et al. (2017):

Note: *The referee comments are given in blue italics.* Our answers are in black. The "Response to Referee #2" is also given in this document starting from the page 12. The revised manuscript with track changes is given after the "Response to Referee #2" (after page 25). Please also be understood that all line numbers mentioned in our answers are referring to the revised manuscript without track changes (given in another file).

Review of gmd-2017-288

PCR-GLOBWB 2: a 5 arc-minute global hydrological and water resources model Sutanudjaja et al.

Summary:

———

This is a well-written manuscript that describes the components of PCR-GLOBWB 2 and its updates since version 1. It also includes an evaluation of a global application of the model at 5 and 30 arc-minute. While no individual component of the model is entirely new (i.e. most of the components have been the subject of their own publications), this manuscript serves a useful purpose in providing a complete overview of the updated model. As such, I recommend that the manuscript is acceptable for publication in GMD pending minor revisions.

We would like to thank Referee #1 for her/his kind appraisal for our paper and valuable suggestions and comments. We concur the importance of this paper to provide a formal and complete overview of our PCR-GLOBWB 2 model that has been used in many studies.

Comments:

———

l.68: 'om' should read 'on'

Thank you for pointing this. We have corrected it in the revised paper.

l.73: What does 'global water management' mean? Most water management decisions are made locally or regionally (e.g. by basin). It is not clear to me which water management decisions are made globally.

We rephrased the sentence to: "These applications show that GHMs have become invaluable tools in support of global change research and environmental assessments."

l.86-88: How many of these publications had someone not closely affiliated with the Utrecht group as their primary authors?

A recent search on Scopus (13 April 2018) using the key-word "PCR-GLOBWB" yielded 113 publications with collectively over 2500 citations. There are 50 publications (44%) without authors from our group (i.e. by excluding "Utrecht University" during the search on Scopus).

l.88: 'yielded 97 publications with collectively over 2100 references'. I assume you mean citations rather than references (since it would be easy to add more references to a paper).

We modified it accordingly.

l.104-106: Is the resolution relevant from a code-perspective? I assume that the code itself is resolution-agnostic and that the resolution of the application is specified in configuration and other input files?

Indeed, the reviewer is right. The resolution is specified in configuration and other input files. We rephrase the sentence to the following (see also lines 104-106 of the revised manuscript without track changes).

"The new version of the model, PCR-GLOBWB 2, which is able to simulate the water balance at a finer spatial resolution of 5 arc-minutes, supersedes the original PCR-GLOBWB 1, which has a resolution of 30 arc-minutes only."

l.119: The experiments described in the manuscript serve to 'evaluate' the model rather than to 'validate' it.

We modified it accordingly. In the revised manuscript, the terms "validation", "validate", and "validated" were not used. They have been replaced replaced with "evaluation", "evaluate", and "evaluated" (see e.g. lines 117-119 of the revised manuscript).

l.178-179: '[...] in which the exchange of water between a series of interconnected stores is easily performed'. Awkward phrasing. You don't 'perform exchange' and it's unclear what 'easily' means in this context.

We removed the phrase.

l.180: Provide more details on the modular construction of the model at the code level. This is of interest to readers of GMD.

We appreciate the suggestion. However, we think that such details (at the code level) are not beneficial for the manuscript and general readers as they are hardly presented in a concise and straightforward manner. For readers that are interested with the model code, we refer to the PCR-GLOBWB github page https://github.com/UU-Hydro/PCR-GLOBWB_model (in the manuscript, see also Section 5 "Code and data availability").

Nevertheless, regarding to this comment, we add the following sentences to the revised manuscript in order to briefly state our general approach in developing the model code of PCR-GLOBWB 2 (see Section 2.4, lines 48-453 of the revised manuscript without track changes).

"To allow for exchanges of model components and, therefore, evaluate different model configurations, a component-based development approach (e.g Argent, 2004; Castronova and Goodall, 2010) was followed while developing the PCR-GLOBWB 2 model code. Each of the PCR-GLOBWB scientific modules described in section 2.3 is implemented in a separate Python class that needs to implement initialization and update methods. The latter designates changes of states and fluxes per time step. Each of module is initialized and executed by iteratively calling the update method via a main model script."

Figs 1 and 2: Combine into one single figure.

We modified it accordingly.

l.196-210: Provide proper references.

As far as we are concerned, the proper references were already provided. In the revised manuscript, we tried to improve them by putting the link inside the brackets for each reference. This may avoid unnecessary confusion. Please kindly let us know if there are more things that we should do (see lines 182-197).

l.239-240: How are rain-fed crops handled?

The PCR-GLOBWB land cover classes used for a demonstration in this manuscript consist of four land cover classes: 'tall natural vegetation', 'short natural vegetation', 'non-paddy irrigated crops', and 'paddy-irrigation'. Here we simplified that the "rain-fed crops" was merged to the 'short natural vegetation'. Nevertheless, there is also a version (Bosmans et al., 2017) that consists of six land cover classes and handles the "rain-fed crops" in a separate class, albeit still at 30 arc-minute resolution only.

Related to this comment, we have revised the first paragraph of Section 2.3.2 as follows:

"This core module of PCR-GLOBWB 2 covers the land-atmosphere exchange, the vertical flow between soil compartments and the eventual groundwater recharge, snow and interception storage and the runoff generation mechanisms. These processes are simulated over a number of land cover types and aggregated proportionally based on land cover fractions within a model cell. Users can specify their own land cover classification and introduce their own land cover parameterization. The standard parameterization of PCR-GLOBWB 2 carries four land cover types consisting of tall natural vegetation, short natural vegetation, non-paddy irrigated crops, and paddy irrigated crops (i.e. wet rice). There is also a parameterization set for six land cover types (Bosmans et al., 2017), albeit still at 30 arc minute resolution only, that include distinct types for pasture and rain-fed crops. For the standard four land cover parameterization of PCR-GLOBWB, applied in this paper, the land cover types of pasture and rain-fed crops are integrated into the short natural vegetation type."

l.239-240: How easy / hard would it be for users to add additional / different land use types (e.g. urban or tundra)

Users can specify their own land cover classification and introduce their own land cover parameterization (as done by Bosmans et al., 2017). Within our department, although not for global extent simulation, there are also some ongoing studies (e.g. master and phd projects) implementing PCR-GLOBWB 2 with their own customized land cover classes (e.g. separating sugar cane in a separate land cover class in order to assess hydrological impacts of its expansion due to growing bio fuel needs).

l.251: Describe how 'Darcian flow' is implemented. Is this vertical drainage only under unit gradient? How is the unsaturated hydraulic conductivity specified or calculated?

Net vertical fluxes between the stores 1 and 2 are driven by degrees of saturation of both layers, s. They are calculated either as $s_1 = S_1/SC_1$ and $s_2 = S_2/SC_2$; or $s_1 = \theta_1/\theta_{sat,1}$ and $s_2 = \theta_2/\theta_{sat,2}$, where S is the storage, SC is the storage capacity, θ is the effective moisture content defined as the fraction of storage over thickness, and the subscript sat indicates saturation. In principle, net vertical fluxes between both stores, Q_{12} consists of a downward percolation $Q_{1\rightarrow 2}$ and a capillary rise $Q_{2\rightarrow 1}$. If there is enough water in S_1, percolation $Q_{1\rightarrow 2}$ is equal to the first store unsaturated hydraulic conductivity, $K_1(s_1)$. If $s_1 < s_2$, capillary rise may occur with the amount of $Q_{2\rightarrow 1} = K_2(s_2) \times (1-s_1)$, where $K_2(s_2)$ is the second store unsaturated hydraulic conductivity and $(1-s_1)$ is the moisture deficit in the first store. The unsaturated hydraulic conductivity of each layer, K(s), which depends on the degree of saturation s, is calculated based on the relationship suggested by Campbell (1974): $K(s) = Ksat \times s^{2\beta+3}$ where β is a soil water retention curve parameter based on the model of Clapp and Hornberger (1978).

Net vertical fluxes between the second and groundwater stores, Q_{23}, also consist of a downward percolation $Q_{2\rightarrow 3}$ and a capillary rise $Q_{3\rightarrow 2}$. Basically, the fluxes Q_{12} and Q_{23} are calculated in a similar fashion as $Q_{1\rightarrow 2}$ and $Q_{2\rightarrow 1}$ (described above). Yet, the capillary rise $Q_{2\rightarrow 3}$ (from the groundwater store) only occurs in areas with shallow groundwater tables and with a condition that the resulting moisture content in the second layer cannot exceed its field capacity.

In the revised manuscript, we do not want to add this lengthy explanation. Rather, we will put just some references as follows (see lines 242-244).

"In the soil column, vertical fluxes are based on driven by degrees of saturation of soil layers and interact with the underlying groundwater store, S3 (see e.g. van Beek and Bierkens, 2009; Sutanudjaja et al., 2011; Sutanudjaja, 2012 for detailed explanation)."

l.276-278: Are the 'where under natural conditions (without groundwater withdrawal) significant groundwater discharge occurs' dynamically calculated or specified?

This should be specified before executing a (non-naturalized) model run (e.g. by performing a naturalized condition run beforehand). Yet, this setting (to limit river bed infiltration only in areas 'where under natural conditions' (without groundwater withdrawal) significant groundwater discharge occurs) is actually optional in PCR-GLOBWB 2. It was not used in the current demonstration of PCR-GLOBWB 2. Therefore, to avoid confusion, we decided to remove this phrase.

l.287: ': Harbaugh et al., 2000)' should read '(Harbaugh et al., 2000)'

We modified it accordingly.

l.301-302: At what resolution is the 8-point steepest gradient algorithm evaluated? I assume at a higher resolution than 5-min or 30-min, because neither will result in accurate channel networks if the steepest gradient algorithm is applied using cell-average elevations at those resolutions.

Indeed, we derived our local drainage map based on a high resolution 30 arc-sec digital elevation model derived by combining the 30 arc-sec HydroSHEDS (Lehner et al., 2008), the 30 arc-sec GTOPO30 (Gesch et al., 1999) and the 1 km resolution of Hydro1k (Verdin and Greenlee, 1996; USGS EROS Data Center, 2006). Please refer to the lines 341-347 of the revised manuscript.

l.302-303: What happens when river flow is routed in an endorheic basin? Does it create an inland sea or is the water removed from the model?

We simplified that water flowing to endorheic basins is removed (e.g. via evaporation). Please refer to the lines 292-294 of the revised manuscript.

l.304-313: Fix grammar and punctuation. As is, the enumeration and the associated semi-columns make no sense since there are multiple sentences after '2)'.

To fix grammar and punctuation, we modified this part. Please see the first and second paragraphs of Section 2.3.4, particularly the lines 289-310 of the revised manuscript.

l.326: How is reservoir management handled? For example, are releases based on storage targets, rule curves, etc. How are different reservoir purposes addressed, e.g. flood control, hydropower, irrigation.

For the runs demonstrated in the manuscript, we just used a simple and globally uniform reservoir management rule. Reservoir releases are estimated as a function of reservoir relative minimum and maximum reservoir capacities (minResvrFrac and maxResvrFrac) and long term (5 year) average discharge (see e.g. Wada et al., 2014, particularly their Equation 11). The default values, used in our runs, for these limits are globally uniform set to 10% and 75% of reservoir capacities. Yet, users can also set their own customized minResvrFrac and maxResvr that can be spatially and temporarily varying and dependent on reservoir purposes (e.g. hydropower reservoirs may have a higher upper limit up to 90%).

l.329: What is a 'standard' storage-outflow relationship?

What we meant by 'a standard' storage-outflow relationship is that lake outflow is calculated in analogy to the simple weir formula as the discharge over a rectangular cross section (Bos, 1989).

To address these two comments (l.326 and l.329), we added the aforementioned references in the revised manuscript.

l.335: What is 'water type'?

What me meant by 'water type' is related to the classification surface water areas to several water types: river channels, inundated floodplains, lakes and reservoirs. To avoid the confusion, we rephrased the sentence as follows (see lines 325-328 in the revised manuscript).

"All surface water areas, which can be classified into several water types: river channels, inundated floodplains, lakes and reservoirs, are subject to open water evaporation calculated from reference potential evaporation multiplied with factors depending on water types and depths."

Section 2.3.4: Are inter-basin water transfers / diversions represented?

Water diversions and inter-basin transfers are limited to the pre-described 0.5-1 arc degree water allocation zones/service areas. Please refer to the lines 415-422.

Section 2.3.5: It is not clear to me how the irrigation efficiency is used in the model. I understand it can be used to estimate the water demand, but what happens to the water after it is removed from storage or the river network. Is the excess water (the 'inefficient' portion) added to the soil (where it can then contribute to evapotranspiration and return flow), is it directly added to return flows, or something else?

Indeed, the irrigated water is added to the soil and the hydrological conceptualization of the PCR-GLOBWB land surface module (e.g. the improved Arno scheme of Hagemann and Gates, 2003) to determine how much of this water contributes to evaporation and transpiration, direct runoff, interflow and groundwater recharge/baseflow. By applying this, we realize that the simulated irrigation consumption values (withdrawal – return flow) on a day-by-day basis would not be necessarily consistent to the irrigation efficiency values (usually at the country scale), a priori set in the model input, buy they will be approximately similar at longer time scales.

l.399: 'would be rather straightforward to change this'. Explain in one sentence how that would be done.

We removed this phrase. Actually, this is still under development. Yet, although the implementation of this feature may be straightforward, we acknowledge further tests are still needed.

l.403: 'as function' should read 'as a function'

We modified it accordingly.

l.413: 'to use literature fractions of groundwater withdrawal and surface water withdrawal'. Awkward, suggested change: 'to use fractions of groundwater and surface water withdrawal reported in the literature'.

We modified it accordingly.

Section 2.5: Does the model use openmp (shared memory) or mpi parallelization?

No. There is still no openmp/mpi technique used. This is still on our wish list for future development.

l.485: Provide details on the memory constraints.

We removed this part (about 'Windows memory constraints') as this may not be entirely true and still require some investigation. We acknowledge that we have little experiences for running PCR-GLOBWB under a Windows operational system. All PCR-GLOBWB 2 developments are done under Linux (including their tests). Previously, before we submitted the manuscript, we received reports from some users that they were not able to run PCR-GLOBWB 2 in their Windows laptop. Yet, recently, about a month ago, one of our partners reported that he managed to run PCR-GLOBWB 2 in his Windows laptop.

Section 3.1.1: Since neither model implementation was calibrated it makes it a challenging to evaluate the statements that say one version (5-arcmin) is inherently better than the other one (30-arcmin).

We respectfully beg to differ. We have two versions/resolutions (5 arc-minute and 30 arc-minute) of the model with were parameterized similarly in terms of land-cover specific parameters (soil and vegetation properties) and sub-grid parameterization of surface runoff, interflow and groundwater discharge using the same underlying high resolution (30 arc-sec/1 km datasets). Differences are the resolution of topography, catchment outline and drainage network, but they are again obtained from the same underlying dataset (e.g. HydroSHEDS elevation map, GLCC land cover map, GLHYMPS hydrogeological map). So the models are entirely comparable, apart from their resolution. If anything, calibrating the models would actually hide some of the differences between the resolutions because of model fitting that would lead to hiding both resolution errors and conceptual errors in the fitted parameters and would make extrapolation of the results to poorly gauged regions of the world questionable. So we believe that the models can be compared without calibration. Results show that the 5 arc-minutes model performs better. We provide possible reasons for this in the paper, and, in response to the second reviewer, we analyze the reasons behind this improvement a bit further in the revised version, showing that a better representation of the vertical temperature distribution improves performance (this is not intrinsic to PCR-GLOBWB though) and also a better performance in smaller catchments.

l.600: 'scale-consistent' - perhaps 'scale-independent'?

We would like to keep on using the term scale-consistent. Scale-independent pertains to parameters that remain unchanged across scales, while scale-consistent allows parameters to change across scales, but the parameters are derived from basic information in the same manner and they are such that if the fluxes from the finer scale model are aggregated to the scale of the coarser scale model, they are the same as the fluxes directly calculated with the coarser scale model. Scale-consistent thus refers to "representative parameters".

Table 1 and comparison of 5- and 30-arcmin resolutions: One way to reduce difference that may occur because of area mismatches would be to provide fluxes also as a depth per unit area, e.g. mm/year.

We added the values in mm/year (see Table 1).

Section 3.4. and following: When providing error metrics (correlation, KGE, etc.) please provide the timestep at which the metric was calculated.

We revised the manuscript accordingly; see e.g. the first paragraph of Section 3.4.1.

l.643: The term 'hydrological extremes' as used here is a bit misleading. For many of the smaller basins, the time-of-concentration is well less than the timestep used in the evaluation of the error metrics. For example, the monthly flow in a 2000km2 basin is not necessarily related to a flood event.

We agree with the reviewer. We have changed it to the following (see lines 634-637): "This is to test if the model is able to capture the monthly scale and inter-annual anomalies in discharge (i.e. on the monthly scale) when the dominant seasonal trend is removed from observations and simulations".

Section 3.4.2: When comparing with GRACE it makes more sense to scale the simulations to the resolution of GRACE (as is done in the analysis for Figure 8) than comparing the GRACE results directly to the 5- or 30-arcmin results. I suggest removing Figure 7 and the accompanying discussion and to focus on Figure 8 instead.

We partly agree with the suggestion to remove the figure and we would like to respectfully request to keep Figure 7. Although we cannot really compare the absolute trend values of PCR-GLOBWB and GRACE (due to different resolutions), this figure is still particularly important to show the groundwater depleted regions based on PCR-GLOBWB simulation and to check their consistencies with GRACE signals.

Figures 9 and 10: Distinguish the left and right columns in the caption and in figure labels.

We modified them accordingly.

References:

Argent, R. M.: An overview of model integration for environmental applications–components, frameworks and semantics, Environmental Modelling & Software 19 (3): 219–34, doi:10.1016/S1364-8152(03)00150-6, 2004.

Bos, M.G.: Discharge measurement structures, third revised edition, ILRI Wageningen, 1989.

Bosmans, J. H. C., van Beek, L. P. H., Sutanudjaja, E. H., and Bierkens, M. F. P.: Hydrological impacts of global land cover change and human water use, Hydrol. Earth Syst. Sci., 21, 5603-5626, https://doi.org/10.5194/hess-21-5603-2017, 2017.

Campbell, G. S.: A simple method for determining unsaturated conductivity from moisture retention data, Soil Science, 117, 311–314, 1974.

Castronova, A. M. and Goodal, J. L.: A generic approach for developing process-level hydrologic modeling components." Environmental Modelling & Software 25 (7): 819–25. doi:10.1016/j.envsoft.2010.01.003, 2010.

Clapp, R. B. and Hornberger, G. M.: Empirical equations for some soil hydraulic properties, Water Resources Research, 14, 601–604, 1978.

Gesch, D.B., Verdin, K.L., and Greenlee, S.K.: New Land Surface Digital Elevation Model Covers the Earth: Eos, Transactions, American Geophysical Union, v. 80, no. 6, p. 69–70, 1999.

Hagemann, S. and Gates, L.D.: Improving a subgrid runoff parameterization scheme for climate mod- els by the use of high resolution data derived from satellite observations, Climate Dynamics, 21, 349–359, 2003.

Harbaugh, A.W., Banta, E.R., Hill, M.C., and McDonald, M.G., 2000, MODFLOW-2000, the U.S. Geological Survey modular ground-water model -- User guide to modularization concepts and the Ground-Water Flow Process: U.S. Geological Survey Open-File Report 00-92, 121 p

Lehner, B., Verdin, K., and Jarvis, A.: New global hydrography derived from spaceborne elevation data, Eos (Washington. DC)., 89, DOI: 10.1029/2008EO100001, 2008.

Sutanudjaja, E. H., van Beek, L. P. H., de Jong, S. M., van Geer, F. C., and Bierkens, M. F. P.: Large-scale groundwater modeling using global datasets: a test case for the Rhine-Meuse basin, Hydrology and Earth System Science, 15, 2913–2935, 2011.

Sutanudjaja, E. H.: The use of soil moisture remote sensing products for large-scale groundwater modeling and assessment, PhD thesis, Utrecht Univ., Netherlands, 2012.

Verdin, K.L., and Greenlee, S.K.,: Development of continental scale digital elevation models and extraction of hydrographic features. In: Proceedings, Third International Conference/Workshop on Integrating GIS and Environmental Modeling, Santa Fe, New Mexico, January 21-26, 1996. National Center for Geographic Information and Analysis, Santa Barbara, California, 1996.

USGS EROS Data Center: HYDRO1k Elevation Derivative Database, LP DAAC: http://edcdaac.usgs.gov/gtopo30/hydro/, 2006.

Van Beek, L. P. H. and Bierkens, M. F. P.: The Global Hydrological Model PCR-GLOBWB: Conceptualization, Parameterization and Verification, Tech. rep., Department of Physical Geography, Utrecht University, Utrecht, The Netherlands, http://vanbeek.geo.uu.nl/suppinfo/vanbeekbierkens2009.pdf, 2009.

Wada, Y., Wisser, D., and Bierkens, M. F. P.: Global modeling of withdrawal, allocation and consumptive use of surface water and groundwater resources, Earth System Dynamics, 5, 15–40, 2014.

Response to Referee #2's review on the GMD-D paper of Sutanudjaja et al. (2017):

Note: *The referee comments are given in blue italics.* Our answers are in black. The revised manuscript with track changes is given after the "Response to Referee #2". All line numbers mentioned in our answers are referring to the revised manuscript without track changes (given in another file).

Major comments:

The authors compiled their earlier modeling efforts and upgraded the PCR-GLOBWB global hydrological model. This paper consists of two parts, model description and validation. The latter part particularly focused on the comparison between two global simulations of 30 arc min and 5 arc min spatial resolutions. The authors claim that the simulation of finer resolution generally outperforms the other.

I found the former part well written except for some technical issues listed below. I am concerned by the validity of discussion of the latter part. The authors mainly compared the histogram of several hydrological indicators for two spatial resolutions. This straightforward approach is sometimes misleading because the performance improvement in some specific conditions can be exaggerated. For instance, because elevation correction is applied for air temperature, the performance of finer resolution is expected better than the other in snow-dominant mountainous regions. Because the river gauging stations are concentrated in northern mid and high latitudes, the effect tends to contrast the performance of two resolutions. Performance improvement must be evaluated with more careful investigations.

We thank the reviewer for his/her thoughtful comments about the validation with streamflow data. We have taken this comment to heart and looked more carefully into the explanation of the improvement in evaluation statistics between 30 and 5 arc-minute model versions. We have now additionally provided validation statistics for different Köppen-Geiger Climate zones and for GRDC stations with different altitudes. Results are shown hereafter with the specific comments.

Second, the performance of water use estimation is questionable. The results indicate that estimated national water use differs from AQUASTAT by one or two orders of magnitude. Since little discussion is provided to these considerable discrepancies, I'm puzzled how I should take these results. Further clarification and reasonable discussion should be added to the water use section.

We agree with the reviewer that we could have been a bit more critical when discussing the validation results of the water withdrawal data. Upon his/her suggestion we have now added discussion better scrutinizing our results and providing additional explanation of the mismatches. We also suggest what could be improved in the "future work" section. We refer to the specific comments for results on this.

Specific comments

Line 52 "H08 (Hanasaki et al 2008a)": H08 seems recently updated (Hanasaki et al. 2018). The paper may be of interest of the authors because some of the model functions are overlapping with PCR-GLOBWB 2.

Good suggestion. We have added it to the list (see the line 54 of the revised manuscript without track changes).

Line 229 "resulting crop specific potential evaporation": Do the authors estimate potential evaporation of trees as well? If this is the case, "vegetation specific" may look better.

We modified the phrase to: "… resulting land cover specific potential evaporation" (see lines 213-216).

Line 239 "tall natural vegetation, short natural vegetation, irrigated crops and paddyirrigation": How are rainfed crops treated in this model?

See our answer for Referee #1 (regarding l. 239-240).

Line 245 "using a monthly climatology of phenology and crop calendars": If the crop calendars are monthly, crops are always planted at the first day of month and harvested at the last day. Is this the case of this model?

Yes, this is indeed correct. We use a cropping cycle and phenology that is the same for every year, i.e. a climatology based on long-term average temperature and precipitation cycles (see van Beek, 2008; van Beek and Bierkens, 2009 for details). Obviously, phenology and crop cycles depend on climatic conditions, but accounting for that means including a dynamic vegetation and crop growth model. This is certainly on our wish list for future development.

Line 256 "All fluxes are computed per land cover type and balanced with the available storage to arrive. . .": Are storage terms computed independently for each land cover type? For instance, is the soil moisture of natural vegetation different from that of irrigated cropland? If not, how water is balanced with the available storage?

Yes, this is indeed the case. Storage terms are calculated and carried through the simulation per land cover type and only when reported averaged over the cells.

Line 284 "Alternatively, an initial estimate of a fossil, i.e. a non-actively replenished, groundwater store can be imposed that provides a similar functionality": Hard to read. Rephrase.

Replaced by: "As an alternative, it is also possible to limit the maximum volume of non-renewable groundwater that can be extracted." (see lines 274-275 in the revised manuscript without track changes).

Line 365 "the crop composition (which changes per month and includes multicropping)": Same question as above. If the crop calendar used is monthly, does it mean all the crops are planted and harvested at the first and the last day of month globally?

Yes, this is the case. See the answer to the question regarding Line 245.

Line 378 "the irrigation water demand is increased by 40% to obtain gross irrigation water demand": Is there any rationale for this coefficient? In Section 3.4.3, the authors simply attributed the underestimated irrigation water withdrawal to this coefficient

Thank you for pointing this out. We found out that this statement was in error. We used country-specific irrigation efficiency values following Rohwer et al. (2007).

We change this sentence to (see lines 369-371):

"The net irrigation demand is augmented to account for limited irrigation efficiency and losses. In PCR-GLOBWB to obtain irrigation water demand including losses, i.e. gross irrigation demand, net irrigation water demand is multiplied with $(1 + f_l)$, with f_l a country-specific loss factor obtained from Rohwer et al. (2007)."

Line 383 "the gross demand and net demand are prescribed to the model and calculated using separate script": Confusing. Are gross and net demand prescribed or calculated?

Both are prescribed. We have removed the part "using separate scripts" as this may be confusing.

Line 445 "2.4 Differences between PRC-GLBWB 1 and 2": This section seems better to be placed after "2.5 Model code".

We have moved the section as suggested.

Line 469 "tailor-made built-in hydrological function": Hard to read. What does it mean?

We changed "tailor-made" by "pre-existing" (see lines 439-441).

Line 470 "its syntax that reads like pseudo-code, generally results in short and readable model codes. . .": Sounds a bit subjective. Describe objective characteristic of code.

We have change "short and readable" with the more objective term "concise" (see lines 439-441).

Line 505 "Note that parameterizations were derived directly following their source data sets using hydrological concepts described in Van Beek and Bierkens (2009)": "The way of setting hydrological parameters are unchanged from Van Beek and Bierkens (2009)"? Is this what the authors meant here? Anyway, it includes little useful information. On what parameterizations do the authors discussing here?

We agree that this may be confusing. We have changed this part to (see lines 499-502):

"The parameterization was mostly unchanged from that given in van Beek and Bierkens (2009), but newer datasets were used if available, such as the GRAND (Lehner et al., 2011) dataset for reservoirs and MIRCA (Portmann et al., 2010) for crop areas."

Line 515 "We used ERA40 and ERA-I results that had been resampled by ECMWFs resampling scheme from their original resolutions to 30 arc-minutes": What do you mean by resampling? Is this different from spatial interpolation? Elaborate methodology and some reasons for adopting the technique.

Resampling means in fact a downscaling technique whereby the values of the larger cells are assigned to the cell centers and then spatially interpolated using inverse distance interpolation. We changed the sentence to (see lines 510-513).

"We used ERA40 and ERA-I results that had been resampled by ECMWFs resampling scheme from their original resolutions (~1.2º and ~0.7º) to 30 arc-minutes. Here, resampling means a form of spatial downscaling whereby the values of the larger ERA40 and ERA-I grid cells are assigned to the cell centers and then spatially interpolated onto 30 arc-minute grids."

Line 522 "Equally monthly reference potential evaporation, computed with Penman-Monteith from the CRU data set was. . .downscaled to daily data proportional to Hamon evaporation. . .": It would be better to state the background or key reasons for this procedure. Why didn't you solve the Penman-Monteith equation and directly derive daily potential evaporation by using ERA40 or ERA-Interim?

We have added the sentence (see lines 519-521):

"We elected not to calculate Penman-Monteith reference evaporation directly from the ERA40 and ERA-I data, in order to avoid the large calculation times needed to process the required meteorological values".

By this procedure we only need precipitation and and temperature as daily values from ECMWF and the monthly CRU values.

Line 562 "main river in PCR-GLOBWB": What is the main river?

We have removed "main".

Line 563 "This yielded 5363 stations for the 5 arc-minute simulation, 3910 stations for the 30 arc-minute simulation": I'm interested in the distribution of catchment area of these stations. For instance, the number of station for 30 arc-minute is smaller than 5 arc-minute one. Is this mainly because the stations below ~2500 km2 of catchment area (an approximate area of a single grid cell) cannot be represented by 30 arcminute? To answer such questions, why don't you show the maximum, minimum, mean, and median of catchment area for each spatial resolution?

The reason is not the minimum size of 2500 km2, but the first criterion: "allowing a not more than 15% difference in catchment area between PCR-GLOBWB 2 and the area reported with the GRDC discharge station". Because catchments sizes differ between resolutions, this criterion results in different results. It is a good suggestion to provide the catchments sizes. We now mention these numbers in the text (see lines 560-562):

5 arc-minutes: min=28.2km2 median=2729.9km2 max=4.68e+6km2
30 arc-minutes: min=31.0km2 median=6560.0km2 max=4.68e+6km2

The small minimum size for the 30 arc-minutes resolution seems to be at odds at first sight. However, we have a Lat-Lon grid, which makes even the 30 arc-seconds cells very small for high latitudes. So, small catchments in high latitudes (mostly the Arctic) can be resolved with 30 arc-minute cells.

Line 602 "regionalization": What is this? Do you mean optimization (or tuning) of hydrological parameters to reproduce historical records?

"Regionalization" is a term mentioned by Samaniego et al. (2017) themselves. It means creating spatially variable parameter fields at the required resolution. We have added "(creating spatially variable parameter fields)" to explain in the text (see lines 597-600).

Line 603 "scale-consistent flux-preserving": Hard to know what is meant here. Rephrase.

Rephrased to "parameterizations that yield the same hydrological fluxes at different resolutions." (see lines 597-600).

Line 604 "parameterization is possible": What kind of parameterization is mentioned here? What does possible mean?

This part has been removed due to the change mentioned under 603.

Line 623 Table 1: It is interesting to compare with earlier works (e.g. Table 2 and 5 of Hanasaki et al. 2018).

We have added the results of Hanasaki et al. (2018) to Table 2.

Line 635 "cross-correlation": Which did you use cross-correlation (a technique frequently used in signal processing) or Pearson's correlation? I'm asking this because the results indicate the authors used Pearson's correlation, but they always wrote cross-correlation throughout the text.

Indeed, we used Pearson's correlation coefficient. We used cross-correlation because we are comparing two time series (measured and simulated) as opposed to autocorrelation. Several of the authors have done time series modelling (Box and Jenkins modelling) before, hence the use of this term. However, as it seems confusing we have removed "cross" and just use "correlation" in the revised manuscript.

Line 647 "Figure 3": It is hard to see the differences between a (30min) and b (5min). Why don't you show the difference between two?

This is a valid point. We now show the correlation coefficient of 5 arc-minute in panel (a) and the difference between 5 arc-minute and 30 arc-minute in panel (b). Please check Figure 2 in the revised manuscript).

Line 648 "Figure 4": As Figure 3 clearly indicates, the selected GRDC stations are concentrated in Europe. Figure 4 might be a bit misleading if the majority of stations are concentrated in some specific regions (e.g. snow dominated stations in Europe). My suggestion is to make Figure 4 for major climatic zones. It would be useful to identify in which climatic conditions the results are improved. As mentioned above, it would be also interesting to separate Figure 4 by catchment area. I suspect the improvements are concentrated in relatively small basins. Another point is that total frequency apparently far exceeds the number of stations (3597). Elaborate how to see these panels (same for Figure 5).

Starting with the total frequency: we thank the reviewer for noting this plotting error which we now corrected. Also, as a result of this error we wrongly plotted the different catchment sizes in the histograms, which we also corrected.

Upon the suggestion of the reviewer we have calculated the measures for different climate zones. We have classified the stations to the Köppen-Geiger climate zones A (Tropical), B (Desert), C (Temperate) and D (Continental). We have excluded the arctic climates as we have hardly any GRDC stations for these regions. We have calculated for each zone the cumulative distribution of the KGE values and plotted the result from the 5 and 30 arc-minutes simulation in one figure for easy comparison. As can be seen from the figures below, the improvement is equally visible climate zones A, B and C and less so for D. Climate zone D is somewhat under-represented in the dataset due to the low densities over Russia, but well represented in the U.S. So, it may indeed be that the improvement is somewhat biased because of the under-representation of the continental zone in the GRDC dataset. We have added a sentence to this effect.

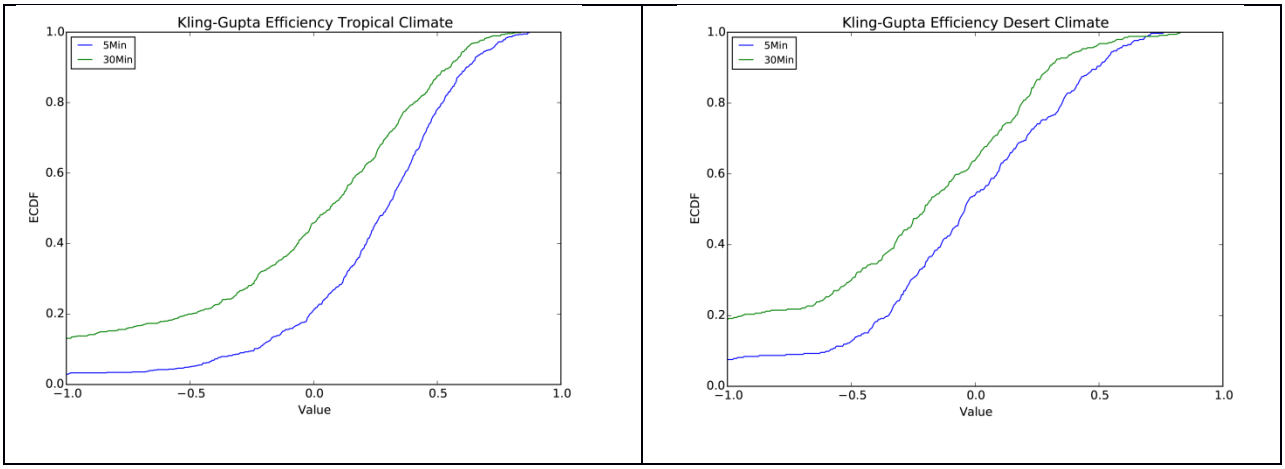

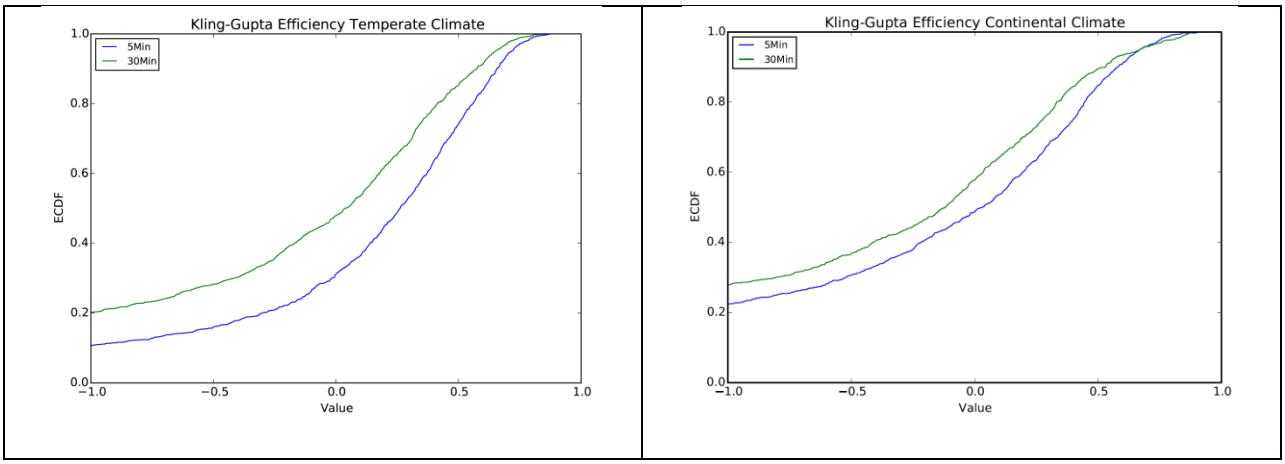

We also checked if the effect of altitude is important in explaining the differences between the 5 and 30 arc-minutes results. The Figure below shows that this is indeed important. The improvements are notable better for GRDC stations at higher altitude than at lower altitude.

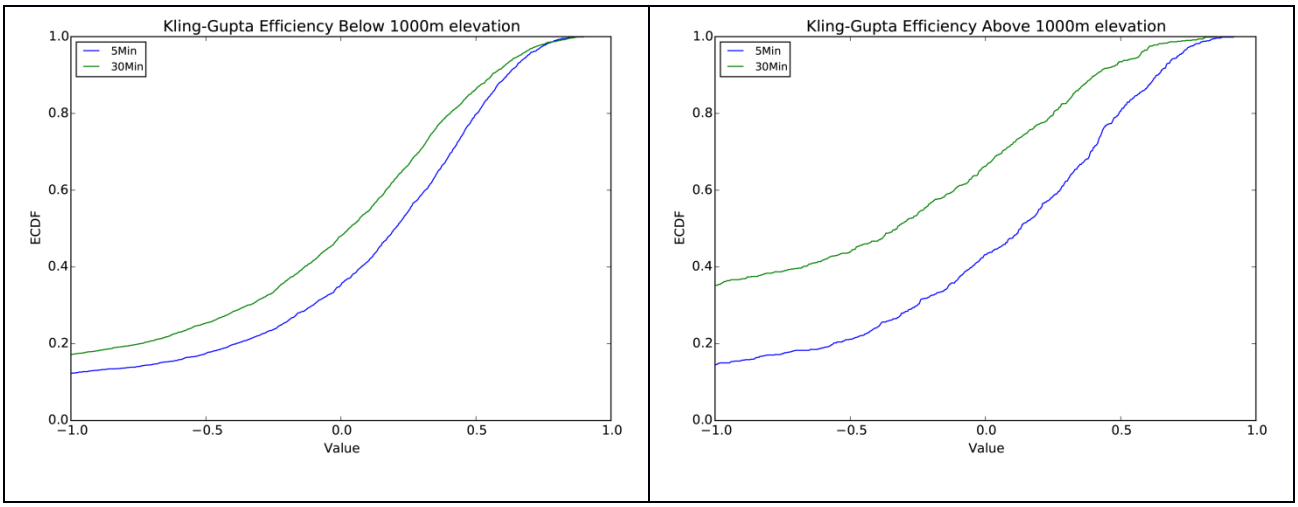

So the resolution has an effect on catchments that are positioned higher because together with the temperature lapse rate, the snow dynamics are better captured at higher resolution.

Finally, in the new plots (see the revised paper) it is now evident that indeed we see a shift to higher KGE and correlation coefficients for the smaller catchments in particular.

So, based on these analyses we changed the paper as follows. In order to limit the paper size we decided not to include the relation between KGE and climate zones, but shortly mention the results of this analysis. We have however included the figure comparing the KGE cumulative distribution plots for GRDC stations below and above 1000 meter and have added comments about the impact of catchment size.

Apart from a new figure (Figure 4 in the revised manuscript), the explanation for the differences between 5 and 30 arc-minutes now reads (see lines 650-667).

"It is difficult to exactly assess which of these factors are most important in determining the improvement. Inspecting the histograms of correlation and KGE (Figure 3) shows that the improvement is mostly apparent for the smaller sized catchments, which supports the notion that a better delineation of the catchments' shape, topography and drainage network could be the cause. However, disentangling these individual effects would require further study. To investigate the possible effects of better snow dynamics we classified the GRDC stations into stations below 1000 m altitude (above mean sea-level) and those above 1000 m. The GRDC stations above 1000 m are expected to experience precipitation falling as snow during periods of the year. The Results in Figure 5 clearly show that the improvement is larger for the higher GRDC stations, This supports the explanation that better snow dynamics due to temperature lapsing in combination with a better resolved digital elevation model is partly responsible for the better results at 5 arc-minutes. We also investigated if improvements were notably different between climate zones, by separately calculating KGEs for GRDC stations in the Köppen-Geiger zones A (Tropical), B (Desert), C (Temperate) and D (Continental). The results (not shown) show that the improvement is equally visible for climate zones A, B and C and less so for D (continental). Without further analysis this is difficult to explain. Note however that the continental climate zone is somewhat under-represented in the GRDC dataset due to the low densities over Russia, although it is well represented in the U.S. So, it may be that the global improvements shown in Figure 3 are somewhat positively biased."

Line 694 "in case of the Niger River, not representing the inner delta. . .": Or simply something wrong with input or validation data.

This could indeed be the case, but there is no strong indication for this. Looking for an explanation, we would rather look at the model itself. We know that floodplain inundation and evaporation is important in the Niger inner Delta and that we have not accounted for it in the simulation. So, this would be the prime candidate for an explanation of the lack of improvement.

Line 653 "a better delineation of the outline of the basins. . .": You mentioned that the error in catchment area is less than 15% for all basins for either spatial resolutions. Further elaborate what do you mean by "better delineation of the outline" here.

We mean a delineation of the "shape" of the catchment. The size could be well represented, but still there could be errors in the shape. We have changed "outline" to "shape" in the revised manuscript (see line 644-654).

Line 656 "better snow dynamics due to the downscaling of temperature to 5 arc-minute resolution": Similar comment to above. This argument must be easily supported by showing the performance of snow dominated regions for two simulations (i.e. excluding snow free regions from Figure 4).

This argument is now supported by an extra figure (see remarks above).

Line 670 "Although results are generally better, the spatial distribution of results is similar to those found by Van Beek et al. (2011) for PCR-GLOBWB1". This conveys hardly any information. What does "generally better" mean? What are similar and what are not?

We agree that this does not add much and removed the sentence.

Line 688 "indicating a higher skill with regard to capturing extremes and anomalies": I'm not convinced at all. As mentioned above, the performance must be different by catchment area, climate, topography and other factors. Show concrete evidences for this claim.

We have already shown the relationships between performance and catchment area, climate and topography. Here we deal with the anomaly correlation, which is the correlation after the mean seasonal variation has been removed. Out of necessity this explains the ability of the model to represent extremes (within-year differences from seasonal averages) and (inter-annual) anomalies. The Figure shows that results are better for the 5 arc-minute simulation. So, the statement as such is correct. We agree that it is difficult then to further explain why anomalies are better captured by the high-resolution model.

Line 763 "Also, Figure 10 shows that agricultural water withdrawal is underestimated . . .": I'm quite puzzled by the right panel of Figure 10a. First, majority of plots are located far below the y=x line indicating most countries are underestimated one (or two) order of magnitude. Next, although majority of countries are strongly underestimated, the correlation slope is larger than 1 which indicates the overall results are overestimated due to some outliers' behavior. These points should be more highlighted to call readers' attention. Finally, my honest interpretation of Figures 9 and 10 is that this model fails to reproduce the historical dynamics of country-specific water withdrawal. At best, the simulation outputs are considerably different from AQUASTAT. Further clarify the authors' intention to show Figures 9 and 10 together with discussion on the capability and limitation of the water use module of PCR-GLOBWB 2.

We agree, as stated in the beginning of this rebuttal, that we could have been a bit more critical when discussing the validation results of the water withdrawal data. We will do so subsequently and also in the manuscript. We respectfully disagree with the statement that the model "fails to reproduce the historical dynamics" which is much too strong. We capture the most important water users by source

and also for irrigation water use, including the increase thereof over the years. Also, we really should mention that none of the previous references shown in e.g. Table 2 have compared water withdrawal to AQUASTAT data *per year, per country per sector and per water source*. Per sector only total water withdrawal has been compared and per country the source of water (Wada et al., 2014). Nevertheless, we should say that:

1) We underestimate groundwater withdrawal for the smaller water users, which can be explained by groundwater use by farmers in summer time for countries for which areas are not registered as irrigation in MIRCA, e.g. Germany and the Netherlands, but which are reported in AQUASTAT.
2) We underestimate irrigation water use for the smaller water users. This is related to the fact that in many of the smaller water use countries, water is used for irrigation only occasionally in dry summers. Thus these areas are not mapped as irrigated crops in MIRCA, or they use irrigation technology that is not part of MIRCA, e.g. subsurface drainage by artificially high surface water levels such as in a number developed delta regions in the world. The fact that these smaller countries are not well represented still means that we are able to capture the big water users, which are most important for global scale analyses. The fact that the slopes are still close to one in Figure 10 comes from the fact that the regression lines have been fit at the original scale and the resulting high leverage of the big users (see the Figure below). We have kept it this way, because we do want to stress the importance to be able to simulate the large quantities of water withdrawal that impact the hydrological cycle significantly.

a) Country water withdrawal for agricultural demand (km3/year) - linear scale

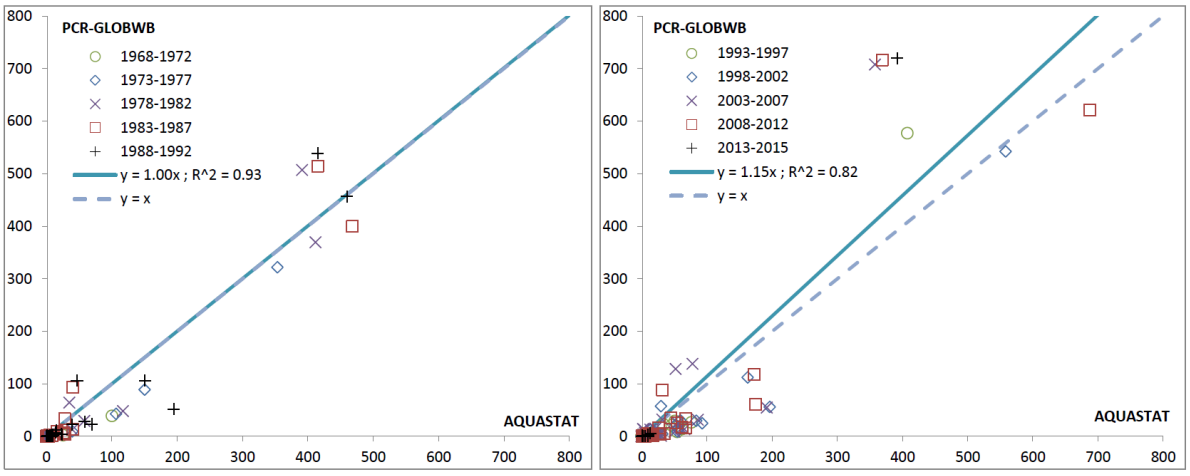

3) The underestimation of industrial water withdrawal is caused by the fact that we do not include water withdrawal for thermo-electric cooling of power plants.
4) The underestimation of domestic water withdrawal comes from the fact that we assume that the priority of water allocation is proportional to demand. This means that in times of shortage, water withdrawal is reduced with and equal percentage for agriculture, industry and domestic. In many countries however, there is a priority series, whereby domestic demand is first met, industrial demand next and agricultural demand comes last. As a result, we underestimate withdrawal. This is also partly the cause for the underestimation of industrial water withdrawal. This is corroborated by

plotting gross water demand (which would be withdrawal if no shortage would occur) against Aquastat data that show a much better fit with regression coefficients closer to 1 for domestic water demand (see the figures below). This shows that improvements are in order in our water allocation scheme.

Accordingly, the description of Figures 9 and 10 now read as follows (see lines 782-813).

"We compared simulated water withdrawal data from PCR-GLOBWB 2 with reported withdrawal data per country from AQUASTAT (FAO, 2016). The results are shown subdivided per source (Figure 10) and per sector (Figure 11). Total water withdrawal and surface water withdrawal are simulated reasonably well (R2 between 0.84 and 0.96 and regression slopes between 0.70 and 1.08). However, groundwater withdrawal is underestimated for the smaller water users. A likely explanation for this is occasional groundwater withdrawal by farmers during dry periods in areas that have not been mapped as irrigated crops in MIRCA, such as grasslands in e.g. Germany and the Netherlands, while this groundwater withdrawal is reported in AQUASTAT.

When looking at water withdrawal per sector, results are mixed. The largest agricultural water users are well captured, but the smaller ones are clearly underestimated. This is related to the fact that in many regions of the smaller water use countries, water is used for irrigation only occasionally during dry summers, while these areas are not mapped as irrigated crops in MIRCA. Also, many of these countries use irrigation technology that is not part of MIRCA, e.g. subsurface drainage by artificially high surface water levels such as in a number developed delta regions in the world. However, even though these smaller countries are not well represented, PCR-GLOBWB 2 is still able to capture the big water users, which have a significant impact on the water cycle and are most important for global scale analyses.

Both industrial and domestic water withdrawals are underestimated. The underestimation of industrial water withdrawal is partly caused by the fact that we do not include water withdrawal for thermo-electric cooling of power plants. The underestimation of domestic water withdrawal comes from the fact that we assume that the priority of water allocation is proportional to demand. This means that in times of shortage, water withdrawal is reduced with an equal percentage for agriculture, industry and domestic use. In many countries however, there is a priority series, whereby domestic demand is first met, industrial demand next and agricultural demand comes last. As a result, we underestimate domestic water withdrawal and it also partly causes the underestimation of industrial water withdrawal. This is corroborated by plotting gross water demand (which would be withdrawal if no shortage would occur) against AQUASTAT data. These plots (not shown here) result in the regression slopes of 0.68-0.75 for industrial demand and 0.78-0.92 for domestic demand. These results thus reveal that the water allocation scheme of PCR-GLOBWB 2 should be further improved."

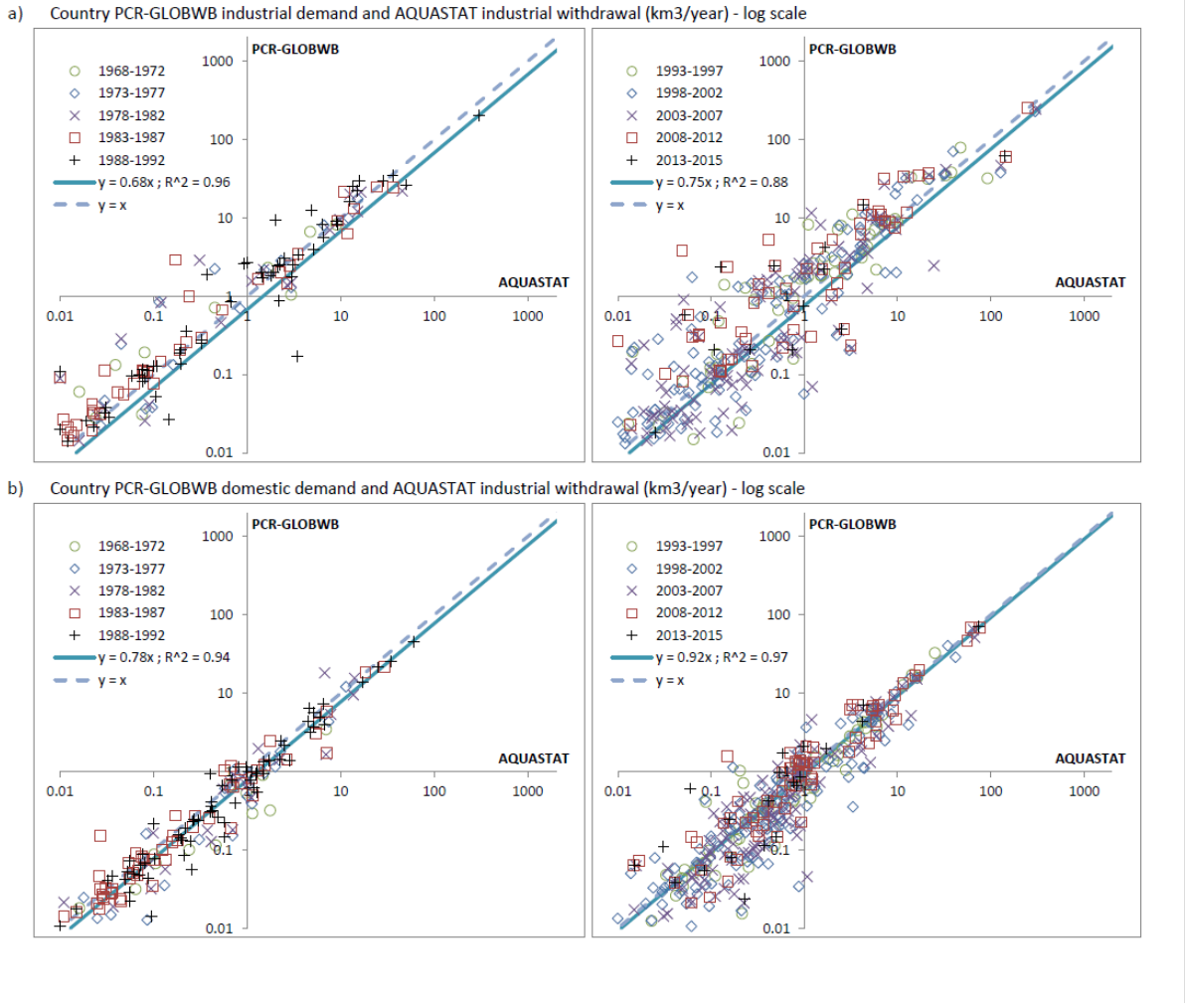

Line 786 "Simulated water withdrawal, by source and sector, matches reasonably well with reported water withdrawal from AQUASTAT": I'm not able to agree with this statement.The authors reported that the regression slope was as low as 0.54 for some cases (line 761).

Agreed. See the previous points.

Technical comments

Line 67 "Schewe et al. 2013; Haddeland et al. 2013": Check publication year of these articles. It must be 2014.

Changed accordingly

Line 89 "collectively over 2100 references": do you mean citations?

Yes. We have changed this accordingly.

References:

Haddeland, I., Heinke, J., Biemans, H., Eisner, S., Flörke, M., Hanasaki, N., Konzmann, M., Ludwig, F., Masaki, Y., Schewe, J., Stacke, T., Tessler, Z. D., Wada, Y., and Wisser, D.: Global water resources affected by human interventions and climate change, P. Natl. Acad. Sci. USA, 111, 3251-3256, 10.1073/pnas.1222475110, 2014.

Hanasaki, N., Yoshikawa, S., Pokhrel, Y., and Kanae, S.: A global hydrological simulation to specify the sources of water used by humans, Hydrol. Earth Syst. Sci., 22, 789-817, 10.5194/hess-22-789-2018, 2018.

Rohwer J, Gerten D, Lucht W. Development of functional irrigation types for improved global crop modelling. PIK Report 104, 2007.

Schewe, J., Heinke, J., Gerten, D., Haddeland, I., Arnell, N. W., Clark, D. B., Dankers, R., Eisner, S., Fekete, B. M., Colón-González, F. J., Gosling, S. N., Kim, H., Liu, X., Masaki, Y., Portmann, F. T., Satoh, Y., Stacke, T., Tang, Q., Wada, Y., Wisser, D., Albrecht, T., Frieler, K., Piontek, F., Warszawski, L., and Kabat, P.: Multimodel assessment of water scarcity under climate change, P. Natl. Acad. Sci. USA, 111, 3245-3250, 10.1073/pnas.1222460110, 2014.

Van Beek, L. P. H.: Forcing PCR-GLOBWB with CRU data, Tech. rep., Department of Physical Geography, Utrecht University, Utrecht, The Netherlands, http://vanbeek.geo.uu.nl/suppinfo/vanbeek2008.pdf, 2008.

Van Beek, L. P. H. and Bierkens, M. F. P.: The Global Hydrological Model PCR-GLOBWB: Conceptualization, Parameterization and Verification, Tech. rep., Department of Physical Geography, Utrecht University, Utrecht, The Netherlands, http://vanbeek.geo.uu.nl/suppinfo/vanbeekbierkens2009.pdf, 2009.

Wada, Y., Wisser, D., and Bierkens, M. F. P.: Global modeling of withdrawal, allocation and consumptive use of surface water and groundwater resources, Earth System Dynamics, 5, 15–40, 2014.

Manuscript prepared for Geosci. Model Dev.
Date: 12 ~~November 2017~~0 May 2018

PCR-GLOBWB 2: a 5 arc-minute global hydrological and water resources model

Edwin H. Sutanudjaja[1], Rens van Beek[1], Niko Wanders[1], Yoshihide Wada[1,2], Joyce H.C. Bosmans[1], Niels Drost[3], Ruud J. van der Ent[1], Inge E. M. de Graaf[4], Jannis M. Hoch[1,5], Kor de Jong[1], Derek Karssenberg[1], Patricia López López[1,5], Stefanie Peßenteiner[6], Oliver Schmitz[1], Menno W. Straatsma[1], Ekkamol Vannametee[7], Dominik Wisser[8], and Marc F. P. Bierkens[1,9]

1 Department of Physical Geography, Faculty of Geosciences, Utrecht University, Utrecht, The Netherlands
2 International Institute for Applied Systems Analysis, Laxenburg, Austria
3 Netherlands eScience Center, Amsterdam, The Netherlands
4 Chair of ~~f~~r Environmental Hydrological Systems , University of Freiburg, Freiburg, Germany,
5 Unit Inland Water Systems, Deltares, Delft, the Netherlands
6 Department of Geography and Regional Science, University of Graz, Graz, Austria
7 Department of Geography, Chulalongkorn University, Bangkok, Thailand
8 Center for Development Research, University of Bonn, Bonn, Germany
9 Unit Soil and Groundwater Systems, Deltares, Utrecht, The Netherlands

Correspondence to: E. H. Sutanudjaja (E.H.Sutanudjaja@uu.nl)

Abstract

We present PCR-GLOBWB 2, a global hydrology and water resources model. Compared to previous versions of PCR-GLOBWB, this version fully integrates water use. Sector-specific water demand, groundwater and surface water withdrawal, water consumption and return flows are dynamically calculated at every time step and interact directly with the simulated hydrology. PCR-GLOBWB 2 has been fully rewritten in Python and PCRaster-Python and has a modular structure, allowing easier replacement, maintenance, and development of model components. PCR-GLOBWB 2 has been implemented at 5 arc-minute resolution, but a version parameterized at 30 arc-minute resolution is also available. Both versions are available as open source codes on https://github.com/UU-Hydro/PCR-GLOBWB_model. PCR-GLOBWB 2 has its own routines for groundwater dynamics and surface water routing. These relatively simple routines can alternatively be replaced by dynamically coupling PCR-GLOBWB 2 to a global two-layer groundwater model and 1D-2D-hydrodynamic models, respectively. Here, we describe the main components of the model, compare results of the 30 arc-minute and the 5 arc-minute versions and evaluate their model performance using GRDC discharge data. Results show that model performance of the 5 arc-minute version is notably better than that of the 30 arc-minute version. Furthermore, we compare simulated time series of total water storage (TWS) of the 5 arc-minute model with those observed with GRACE, showing similar negative trends in areas of prevalent groundwater depletion. Also, we find that simulated total water withdrawal, ~~by source and sector,~~ matches reasonably well with reported water withdrawal from AQUASTAT, while water withdrawal by source and sector provide mixed results.

1 Introduction

The last decades saw the development of an increasing number of global hydrological models (GHMs), e.g. VIC (Liang et al., 1994; Nijssen et al., 2001), WMB (Fekete et al., 2002), WaterGAP (Döll et al., 2003), H08 (Hanasaki et al., 2008a; Hanasaki et al., 2018), MAC-PDM (Gosling and Arnell, 2011) (see Bierkens et al., 2014, Bierkens, 2015 and Kauffeldt et al. 2016 for a more extensive list, also including land surface models). GHMs have become essential tools to quantify and understand the global terrestrial water cycle, as they simulate the distributed hydrological response to weather and climate variations at higher resolution (typically $0.5^{o}\times0.5^{o}$) than used previously in general circulation models (GCMs), with more sophisticated runoff generation processes and river routing. As such, global hydrological models have been used for medium-range to seasonal flood forecasting (Bierkens and van Beek, 2009; Alfieri et al., 2013; Candogan Yossef et al., 2013) as well as for a myriad of water-related global change assessments. Examples are: the projection or estimation of future flood and drought events (Sperna-Weiland et al., 2012; Dankers et al., 2013; Prudhomme et al., 2013, Wanders et al. 2015, Wanders and Wada, 2016), current and future flood hazard and risk (Pappenberger et al., 2012; Hirabayashi et al., 2013; Ward et al., 2013; Winsemius et al., 2013; 2016), global groundwater depletion (Wada et al., 2010; Gleeson et al., 2012), the contribution of terrestrial water stores to global sea level change (Konikow, 2011; Wada et al., 2012; Pohkrel et al., 2013), current and future water scarcity under climate change and increasing population growth (Hanasaki et al., 2008b; Wada et al., 2011a, 2011b; Schewe et al., 2013~~2014~~; Haddeland et al., 2013~~2014~~; Wada and Bierkens, 2014), tele-connections between climate oscillations and water availability (Wanders and Wada, 2015), the impact of land use change ~~om~~ on global water resources (Rost et al., 2008; Sterling et al., 2015; Bosmans et al., 2017~~6~~) and trends in surface water temperature and cooling water potential (van Beek et al., 2012; van Vliet et al., 2012). More recently, the output from global hydrological models has been extended to study socioeconomic impacts, such as virtual water trade (Konar et al., 2013; Dalin et al., 2017) and future agricultural production (Elliott et al., 2013). These applications show that GHMs have become invaluable tools in support of global change research and environmental assessments. ~~of global water management and policy assessments.~~

PCR-GLOBWB (PCRaster GLOBal Water Balance) (van Beek and Bierkens, 2009; van Beek et al. 2011) is one of the recently developed GHMs. PCR-GLOBWB is a grid-based global hydrological model developed at the Department of Physical Geography, Faculty of Geosciences, Utrecht University, the Netherlands. The model, describing the terrestrial part of the hydrological cycle, was first introduced in a technical report by van Beek and Bierkens (2009) and then formally published in a paper of v~~V~~an Beek et al. (2011), focusing on global water availability issues. PCR-GLOBWB was originally developed to solve the global daily surface water balance with a spatial resolution of 30 arc-minutes (about 50 km by 50 km at the equator) and compare the resulting fresh water availability with monthly sectoral water demand in order to assess global-scale water scarcity (van Beek et al., 2011; Wada et al., 2011a,b). In this first version of PCR-GLOBWB (called PCR-GLOBWB 1 hereafter), similar to other global-scale hydrological models, water demand and water availability are treated independently, i.e.

without direct feedback between human water use and other terrestrial water fluxes (e.g. Döll and Siebert, 2002~~;~~, Wisser et al., 2010). Since it was first introduced, PCR-GLOBWB has been applied extensively in global water resources assessment studies. For instance, a recent search on Scopus (accessed on ~~30~~ 13 ~~October~~ April ~~2017~~2018) on the key-word "PCR-GLOBWB" yielded ~~97~~ 113 publications with collectively over ~~2100~~ 2500 ~~references~~citations. Since the first version, several new model features have been introduced such as a comprehensive water demand and irrigation module (Wada et al., 2011b, 2014), a scheme for dynamic allocation of sectoral water demand to available surface water and groundwater resources and the associated calculation of return flow (de Graaf et al., 2014). These features essentially introduced a two-way interaction between water demand, water withdrawal, water consumption and availability, particularly over irrigated areas where water demand is large and return flow is significant. Nevertheless, all of these preceding studies using PCR-GLOBWB were performed at a relatively coarse resolution of 30 arc-minutes, limiting their sub-regional or local applications. Additionally, some added functionalities, such as the possibility to couple the land surface component of PCR-GLOBWB to a global MODFLOW-based groundwater model (Sutanudjaja et al., 2011~~;~~, 2014~~;~~ de Graaf et al., 2015~~;~~ 2017) and an extension to simulate surface water temperature (v~~V~~an Beek et al., 2012), were incorporated in different versions based on the original PCR-GLOWB 1, leading to divergent model code development.

The objective of this paper is to summarize and present the new version of the model, PCR-GLOBWB 2, which consolidates all components that have been developed since the original version of the model was first introduced (van Beek et al., 2011). The new version of the model, PCR-GLOBWB 2, which is able to simulate~~s~~ the water balance at a finer spatial resolution of 5 arc-minutes ~~and~~, supersedes the original PCR-GLOBWB 1, ~~that~~ which has a resolution of 30 arc-minutes only[1]. The finer resolution of PCR-GLOBWB 2 allows a much better representation of the effects of spatial heterogeneity in topography, soils, and vegetation on terrestrial hydrological dynamics (Wood et al., 2011~~;~~, Bierkens et al., 2014). Likewise, it provides a better resolution for visualization that allows stakeholders and decision makers to assess model simulation output more easily and directly for the places they are specifically interested in (Sheffield et al., 2010~~;~~, Beven and Cloke, 2012). To ~~evaluate~~ assess the possible improvements, this paper also presents the first ~~validation~~ evaluation results from the simulation of PCR-GLOBWB 2 at 5 arc-minute resolution and compares ~~this with~~them to a 30 arc-minute~~s~~ version. As discharge data are commonly used in hydrological model performance evaluation, the simulated river discharge of PCR-GLOBWB 2 is compared to in situ discharge observations from the Global Runoff Data Centre (GRDC, 2014).

The paper is organized as follows. Section 2 provides a global description of PCR-GLOBWB 2, including its model structure and the new components and functionalities that have been added since PCR-GLOBWB 1. In section 3 the global application of PCR-GLOBWB 2 is demonstrated and the results from a 58-year simulation (1958-2015) are ~~validated~~evaluated against observations of discharge, total water storage and reported withdrawal

[1] ~~-~~Note that Wada et al. (2016) made a preliminary version of the model that operates at 6 arc-minutes.

data. Section 4 summarizes and concludes this paper and discusses possible future developments. Section 5 provides information about availability of the model code and the underlying data.

2. PCR-GLOBWB 2 – Model description

2.1 General overview

PCR-GLOBWB 2 is a state-of-the-art grid-based global hydrology and water resources model. It is a component-based model implementation in Python using open source PCRaster Python routines (Karssenberg et al., 2010; http://pcraster.geo.uu.nl/). The code is distributed through Github. The computational grid covers all continents except Greenland and Antarctica. Currently two versions are available: one with a spatial resolution of 5 arc-minutes in latitude and longitude and one with a coarser resolution of 30 arc-minutes. Typical time steps for hydrology and water use are one-day while sub-daily time stepping is used for hydrodynamic river routing. For all dynamic processes involved, PCR-GLOWB 2 uses a time-explicit scheme. For each grid cell and each time step, PCR-GLOBWB 2 simulates moisture storage in two vertically stacked upper soil layers (S_1+S_2 in Figure 1), as well as the water exchange between the soil, the atmosphere and the underlying groundwater reservoir (S_3 in Figure 1). The exchange with the atmosphere comprises of precipitation, evaporation from soils, open water, snow and soils and plant transpiration, while the model also simulates snow accumulation and snowmelt. Sub-grid variability of land use, soils and topography is included and influences the schemes for runoff-infiltration partitioning, interflow, groundwater recharge (from S_2 to S_3) and capillary rise (from S_3 to S_2). Runoff, generated by snowmelt, surface runoff, interflow and baseflow, is routed across the river network to the ocean or endorheic lakes and wetlands. Routing can either be simple accumulation, simplified dynamic routing using a method of characteristics, or kinematic wave routing. In case the kinematic wave routing is used, it is also possible to use a (simplified) floodplain inundation scheme and to simulate the surface water temperature.

PCR-GLOBWB 2 includes a simple reservoir operation scheme that is applied to over roughly 6000 manmade reservoirs from the GranD database (Lehner et al., 2011), which are progressively introduced according to their construction year. Human water use is fully integrated within the hydrological model, meaning that at each time step: 1) water demands are estimated for irrigation, livestock, industry and households; 2) these demands are translated into actual withdrawals from groundwater, surface water (rivers, lakes and reservoirs) and desalinization, subject to availability of these resources and maximum groundwater pumping capacity in place; 3) consumptive water use and return flows are calculated per sector.

As an option PCR-GLOBWB 2 can be partially or fully coupled to a two-layer global groundwater model based on MODFLOW (de Graaf et al, 2017). Recent work (Hoch et al., 2017a,b) also includes coupling PCR-GLOBWB 2

to either Delft3D Flexible Mesh (Kernkamp et al., 2011) or LISFLOOD-FP (Bates et al., 2010) which are model codes that can be used to solve the 1D-2D shallow water equations (or approximations thereof) for detailed inundation studies.

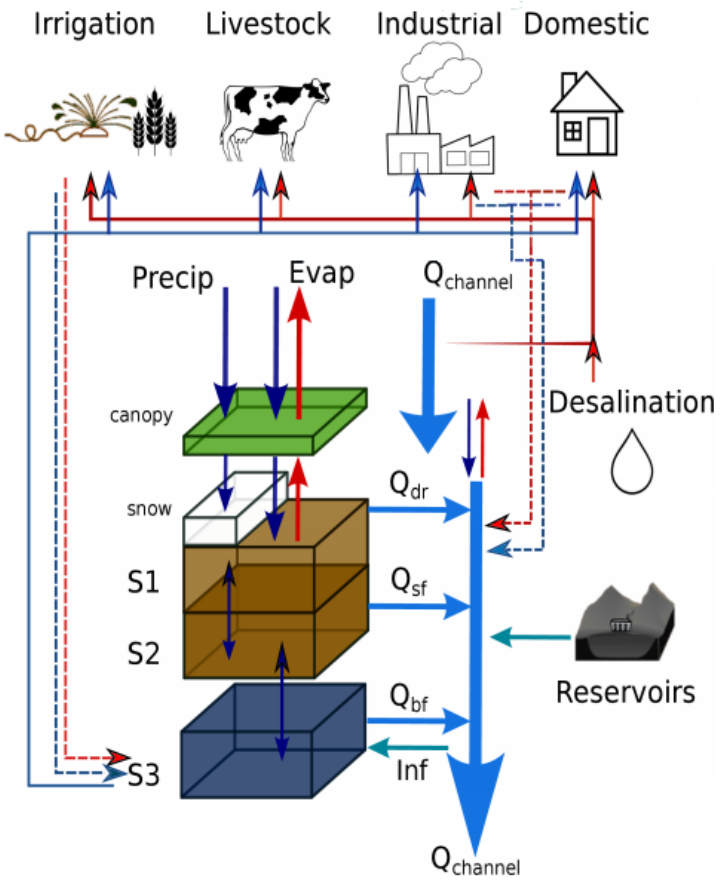

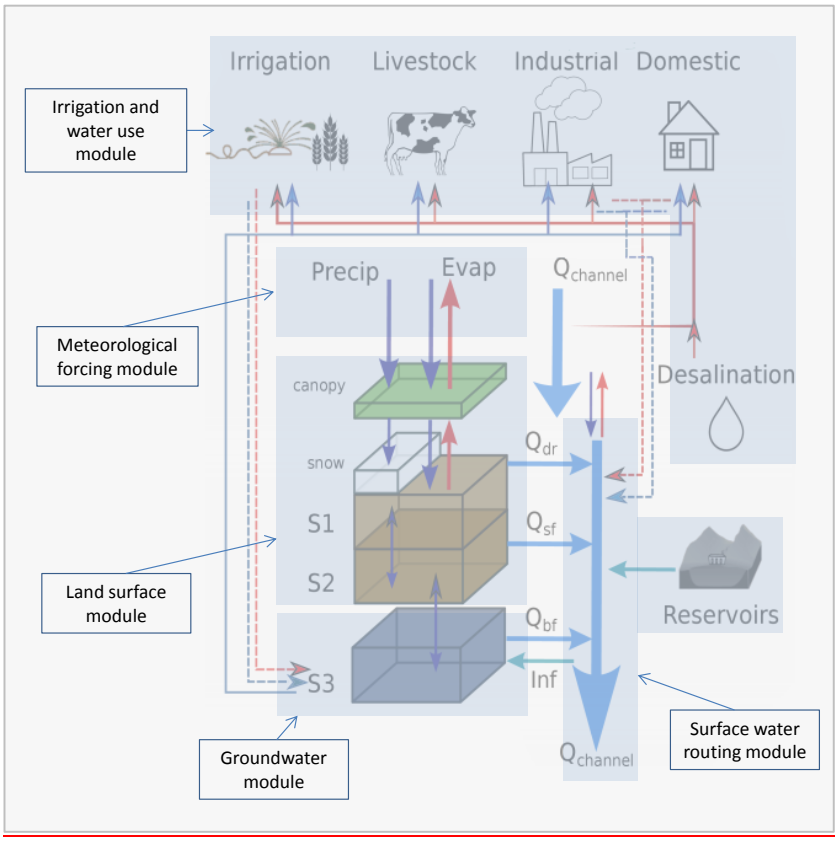

168

169 *Figure 1. Schematic overview of a PCR-GLOBWB 2 cell and its modelled states and fluxes.* S_1, S_2 *(soil moisture*
170 *storage),* S_3 *(groundwater storage),* Q_{dr} *(surface runoff – from rainfall and snowmelt),* Q_{sf} *(interflow or stormflow),*
171 Q_{bf} *(baseflow or groundwater discharge),* Inf *(riverbed infiltration from to groundwater). The thin red lines*
172 *indicate surface water withdrawal, the thin blue lines groundwater abstraction, the thin red dashed lines return*
173 *flows from surface water use and the thin dashed blue lines return flows from groundwater use surface. For each*
174 *sector: withdrawal - return flow = consumption. Water consumption adds to total evaporation.* *In the figure, the*
175 *five modules that make up PCR-GLOBWB 2 is portrayed on the model components.*

176

177

2.2 Model structure and flexibility

PCR-GLOBWB 2 has a flexible modular structure ~~in which the exchange of water between a series of interconnected stores is easily performed~~ (Figure 1).~~)~~ The modular structure of PCR-GLOBWB 2, both in terms of model concepts and implementation (separate modules are called from a main program), makes it easy to modify or replace components according to specific objectives of the model application, to introduce new modules or components within the modelling system and to couple it to existing codes.

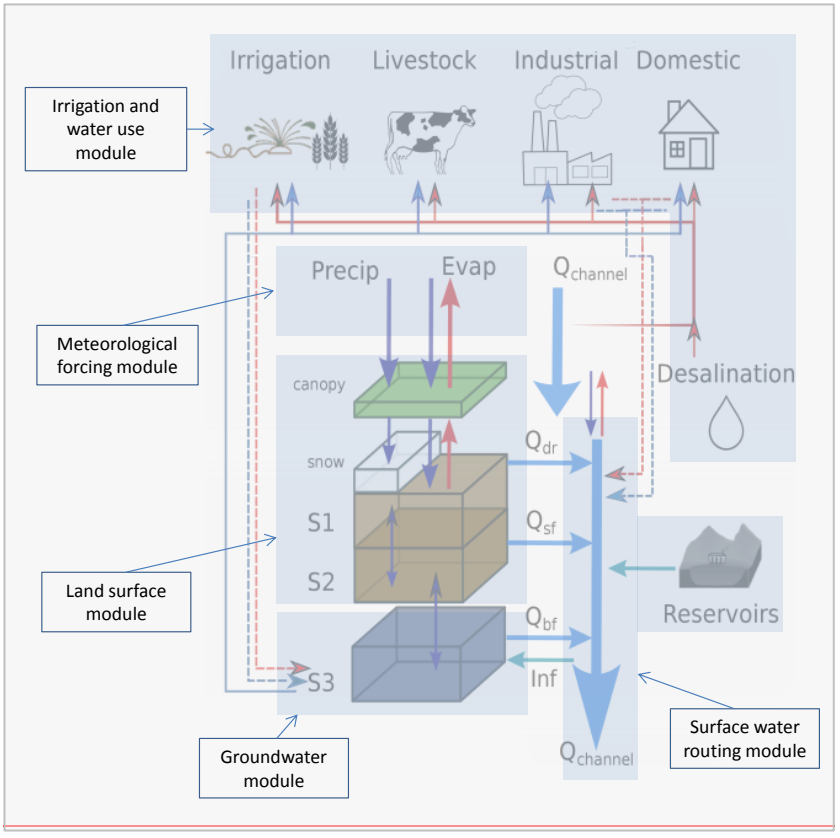

~~*Figure 2. The five modules that make up PCR-GLOBWB 2 portrayed on the model components of Figure 1.*~~

There are currently five main hydrological modules in PCR-GLOBWB 2 as illustrated in Figure ~~2~~ 1 and briefly described in Section 2.3: Meteorological forcing~~;~~, Land surface~~;~~ Groundwater~~;~~ Surface water routing~~;~~ Irrigation and water use. For an extensive description of the underlying equations and methods used in each of these modules we refer to the following sources:

- Meteorological forcing module: van Beek (2008,) http://vanbeek.geo.uu.nl/suppinfo/vanbeek2008.pdf)
- Land surface module, groundwater module and surface water routing module: van Beek and Bierkens (2009), http://vanbeek.geo.uu.nl/suppinfo/vanbeekbierkens2009.pdf ;);, van Beek et al. (2011,) http://dx.doi.org/10.1029/2010WR009791)
- Irrigation and water use module:
    - Calculation of water demand: Wada et al., (2014), https://doi.org/10.5194/esd-5-15-2014)
    - Calculation of water withdrawal, consumption and return flows: de Graaf et al. (2014), https://doi.org/10.1016/j.advwatres.2013.12.002;—);, Wada et al. (2014), https://doi.org/10.5194/esd-5-15-2014);; Erkens and Sutanudjaja (2015), https://doi.org/10.5194/piahs-372-83-2015)

Furthermore: for details about coupling to MOFLOW we refer to:

- One-way coupling: Sutanudjaja et al. (2011), https://doi.org/10.5194/hess-15-2913-2011;);, De de Graaf et al. (2017), https://doi.org/10.1016/j.advwatres.2017.01.011)
- Two-way coupling: Sutanudjaja et al. (2014), http://dx.doi.org/10.1002/2013WR013807)

2.3 Description of the modules

Hereafter, we briefly describe the main features of the five modules. Additionally, a (non-exhaustive) list of the model state and flux variables is provided in Table A1, whereas Table A2 lists the model inputs and parameters, including their sources.

2.3.1 Meteorological forcing module

Meteorological forcing of PCR-GLOBWB 2 uses time series of spatial fields of precipitation, temperature and reference evaporation. Reference potential evaporation can be prescribed or calculated within the model, and is used in the land surface module to calculate land-cover ~~crop~~ specific potential evaporation based on crop factors of the various land cover types according to the FAO guidelines (Allen et al., 1998). There are two options for calculating reference potential evaporation: 1) using Hamon (1963) in case only daily mean temperature is available~~;~~, 2) using Penman-Monteith following the FAO guidelines (Allen et al., 1998) if net radiation, wind speed and vapour pressure deficit are additionally available. See van Beek et al. (2008) for details. The resulting ~~crop~~ land-cover specific potential evaporation is subsequently used to compute the actual evaporation for different land cover types in each cell. Apart from the calculation of evaporation, temperature is also used to partition precipitation into snow and rain and to drive snowmelt.

2.3.2. Land surface module

This core module of PCR-GLOBWB 2 covers the land-atmosphere exchange, the vertical flow between soil compartments and the eventual groundwater recharge, snow and interception storage and the runoff generation mechanisms. These processes are simulated ~~Information is organized per~~ over a number of land cover types and aggregated proportionally based on land cover fractions ~~occupying~~ within a model cell. ~~and the fraction it occupies within a cell.~~ Users can specify their own land cover classification and introduce their own land cover parameterization. The number of land cover types is configurable. ~~; the~~ The standard parameterization of PCR-GLOBWB 2 ~~-~~carries four land cover types ~~:~~ consisting of tall natural vegetation, short natural vegetation, non-paddy irrigated crops ~~(non paddy),~~ and paddy ~~irrigation (i.e., wet rice)~~irrigated crops (i.e. wet rice). ~~The number of land cover types is configurable~~ There is also a parameterization set for six land cover types (Bosmans et al., 2017), albeit still at 30 arc minute resolution only, that includes distinct types for pasture and rain-fed crops. For the standard four land cover parameterization of PCR-GLOBWB, ~~which would also be demonstrated~~applied in this paper, the land cover types of pasture and rain-fed crops are ~~simply~~ integrated into the short natural vegetation type.

~~-~~For each land cover type, separate soil conditions can be specified. It should be noted that the soil and vegetation conditions are in any case fully spatially distributed. Thus, vegetation properties (e.g., crop factor, Leaf Area Index) and soil properties (depth, saturated hydraulic conductivity, etc.) vary not only between land cover types, but may also vary from cell-to-cell (e.g., per climate zone). In the standard parameterization vegetation properties vary over the year using a monthly climatology of phenology and crop calendars (i.e. for the crop factor and LAI).

The application of irrigation water for paddy and non-paddy irrigation is done by the irrigation and water use module. It is based on the FAO guidelines of Allen et al. (1998) and is dependent on the actual soil water storage (S_1, S_2) or paddy-open water storages. All fluxes, from and to the land surface module in Figure ~~2~~1, are thus calculated separately per land cover type. The resulting vertical fluxes for each land cover type are: interception evaporation, bare soil evaporation, snow sublimation, vegetation-specific transpiration. In the soil column, vertical fluxes are ~~based on~~driven by degrees of saturation of soil layers ~~Darcian flow~~ and interact with the underlying groundwater store, S_3.

(see e.g. van Beek and Bierkens, 2009; Sutanudjaja et al., 2011; Sutanudjaja 2012 for detailed explanation).

Surface runoff (Q_{dr}, from precipitation and snowmelt) consists of infiltration excess runoff and saturation excess runoff following a sub-grid approach that mimics variable source areas, i.e. the improved Arno Scheme (Todini, 1996~~;~~, Hagemann and Gates, 2003). Interflow or stormflow (Q_{sf}), mostly occurring in regolith soils on hillslopes, is also handled with a sub-grid approach based on a runoff parameterization by Sloan and Moore (1984). All fluxes are computed per land cover type and balanced with the available storage to arrive at the net flux that is used to update the storages for the next time step. Also, to report the overall fluxes per cell, and to pass these to other modules, the land cover specific fluxes are subsequently averaged (weighted by land cover type fractions).

For the standard parameterization of the land surface module the following data sets are combined (see Table A2): the cell fractions of various non-irrigation land cover types are based on the map of Global Land Cover Characteristics Data (GLCC) Base Version 2.0 (Loveland et al., 2000) with the land cover classification following Olson (1994a~~;~~, b) and the parameter sets from Hagemann et al. (1999) and Hagemann (2002). Irrigation land cover types (i.e. paddy and non-paddy), including their crop calendars and growing season lengths, are parameterized based on the data set of MIRCA2000 (Portmann et al., 2010) and the Global Crop Water Model of Siebert and Döll (2010). We refer to van Beek et al. (2011) for detailed descriptions.

2.3.3. Groundwater module

The groundwater module calculates groundwater storage dynamics subject to recharge and capillary rise (calculated by the land surface module), groundwater discharge (Q_{bf}~~;~~, in case of a positive groundwater storage) and riverbed infiltration (Inf). Groundwater discharge (assumed the same as groundwater baseflow here) depends on a linear storage-outflow relationship ($Q_{bf} = S_3/J$) where the proportionality constant J is calculated following drainage theory of Kraijenhoff-van de Leur (1958) based on drainage network density and aquifer properties. Riverbed infiltration occurs only in case Q_{bf} becomes 0 by groundwater withdrawal~~, and only in areas where under natural conditions (without groundwater withdrawal) significant groundwater discharge occurs~~. Under persistent groundwater withdrawal (calculated with the Irrigation and Water use module) that is larger than the sum of recharge and riverbed infiltration, the groundwater storage S_3 is allowed to become negative. In this case, the part of the withdrawn groundwater in excess of the input (recharge and riverbed infiltration) is seen as non-renewable groundwater withdrawal leading to groundwater depletion (permanent loss of groundwater from storage). In case

withdrawal becomes smaller than the input, the remaining input is used to first fill the negative storage to zero, before baseflow Q_{bf} commences again. As an alternative, it is also possible to limit the maximum volume of ~~-~~non-renewable groundwater ~~-~~that can be extracted. ~~Alternatively, an initial estimate of a fossil, i.e. a non-actively replenished, groundwater store can be imposed that provides a similar functionality~~.

It is possible to use a full-fledged groundwater flow model based on MODFLOW ~~:~~ (Harbaugh et al., 2000) coupled to PCR-GLOBWB 2 in order to calculate groundwater heads and flow paths. This can be done as a one-way coupling where PCR-GLOWB 2 is first run with the standard groundwater module (reservoir S_3 with only vertical fluxes) to yield time series of net groundwater recharge (recharge – capillary rise) and surface water levels. These fluxes/inputs are subsequently used to force the groundwater flow model (see e.g. Sutanudjaja et al., 2011~~;~~, de Graaf et al., 2017). Another possibility is to use a two-way coupling where the groundwater module of PCR-GLOBWB 2 is replaced by the groundwater flow model. In this case, at each time step fluxes are exchanged between the groundwater model and the land surface module, and the groundwater model and the surface water routing module (Sutanudjaja et al. 2014).

2.3.4 Surface water routing module

Following an 8-point steepest gradient algorithm across the terrain surface (local drainage direction or LDD), all cells of the modelled domain are connected to a strictly convergent drainage network that together makes up the river basins and sub-basins of the model domain. The lowermost cell is either connected to the ocean or to an endorheic basin. Per cell, the sum of the three daily runoff fluxes (Figure 1) is aggregated and routed along the drainage network until passing the lowermost cell and being removed from the model. ~~,~~Routing can be done in three ways of increasing complexity: 1) simple accumulation of the fluxes over the drainage network~~,~~; 2) a travel-time characteristic solution (Karssenberg et al., 2007)~~,~~ and 3) the kinematic wave solution.

The first method is typically aggregated over longer time steps (e.g. month or year) that are larger than the travel times of water along the longest river length. The second routing method includes an estimation of cell flow velocity based on average discharge from the last 5 years and ~~;, 2) a travel-time characteristic solution (Karssenberg et al., 2007). Here, for each cell flow velocity is calculated in advance based on bankfull discharge and~~ Manning's equation, which ~~(assuming~~ assumes the energy slope to be equal to the bed slope~~)~~. ~~Next, t~~This estimated velocity is used to move the volume of water in the channel of a cell the corresponding distance within one daily time step along the drainage network. This method works reasonably well for relatively steep rivers in humid climates where the friction slope is close to the bed slope and the rivers are equally filled with water throughout the year~~;, 3)~~. The third method is the kinematic wave approximation of the Saint Venant equations with flow described by Manning's equation~~.~~, Also, here, it is assumed that friction slope and bed slope are equal, which makes it valid for rivers without backwater effects. The kinematic wave is solved using a time-explicit variable

sub-time stepping scheme based on the minimum Courant number. Of these methods, the kinematic wave solution simulates the propagation of the flood wave more realistically while the others provide an expedient means to approximate discharge over longer periods.

Using the kinematic wave method, it is possible to model floodplain inundation which occurs if the discharge exceeds the bankfull capacity of a channel. The excess discharge volume is spread over the entire cell from the lowest part of the cell (based on a higher resolution sub-grid DEM) yielding a flooded area with an approximated flood depth. In case of flooding, the simulated river flow is impacted by adjusting the wetted area and wetted perimeter and calculating a weighted Manning coefficient from the individual Manning coefficients of the floodplains and the channel.

Lakes and reservoirs are part of the drainage network. Lakes and reservoirs can extend over multiple cells, in which case the storage is subdivided by area such as to ensure that lake and reservoir levels are the same across their extent. The active storage of lakes and the actual storage of reservoirs are dynamically updated~~:~~, for the lake outflow a standard storage-outflow relationship based on a rectangular cross-section over a broad-crested weir (Bos, 1989) is used, while reservoirs follow a release strategy. This strategy is, by default, aimed at passing the average discharge, while maintaining levels between a minimum and maximum storage (Wada et al., 2014), but more elaborate strategies that take account of downstream water demand are possible (e.g. v~~V~~an Beek et al., 2011). Lakes and reservoir areas change based on global volume-area relationships. All surface water areas, ~~i.e.~~which can be classified into several water types, ~~the~~ river channels, inundated floodplains, lakes and reservoirs, are subject to open water evaporation calculated from reference potential evaporation multiplied with ~~a~~ factors depending on water types and ~~water~~ depths. Moreover, surface waters are subject to surface water withdrawal calculated with the Irrigation and Water Use module.

If the kinematic wave approach is used, it can be also augmented with an energy routing scheme to simulate surface water temperature (v~~V~~an Beek et al., 2012). Finally, it should be noted that it is possible to run the routing routine from PCR-GLOBWB 2 as a stand-alone routine, which allows it to be fed with the specific discharge from other land surface models.

The routing methods that are available in PCR-GLOBWB 2 will yield significant errors for wide lowland rivers where backwater effects are important. In this case, it is possible to replace the surface water module for part of the modelling domain with hydrodynamic models solving the shallow water equations (Hoch et al., 2017a). Hoch et al. (2017b) developed a generic coupler for this purpose that enables coupling to multiple hydrodynamic modelling codes (https://doi.org/10.5281/zenodo.597107).

Although any data set can be used to define the drainage network and locate the lakes and reservoirs, the standard parameterization of PCR-GLOBWB 2 that runs globally uses the drainage network derived from the high

resolution 30 arc-sec HydroSHEDS (Lehner et al., 2008) combined with 30 arc-sec GTOPO30 (Gesch et al., 1999) and 1 km Hydro1k (Verdin and Greenlee, 1996~~;~~, USGS EROS Data Center, 2006)~~;~~, lakes taken from GLWD~~1~~ (Lehner and Döll, 2004) and reservoirs obtained from GranD (Lehner et al., 2011).

2.3.5 Irrigation and water use module

In PCR-GLOWB 1 water demand was calculated separately from the hydrology and water availability calculated as a post-processing step by subtracting upstream demand (Wada et al., 2011a,b). In PCR-GLOBWB 2 water use (withdrawal and consumption) is fully integrated. Hereafter, the main features of the irrigation and water use module are described in the following order: water demand, water withdrawal, water consumption and return flows.

Water demand

Irrigation water demand is calculated based on the crop composition (which changes per month and includes multi-cropping) and the irrigated area per cell. As stated above, these are obtained from MIRCA2000 (Portmann et al., 2010) and the Global Crop Water Model (Siebert and Döll, 2010). In the standard PCR-GLOBWB 2 parameterization the irrigated areas change over time. In want of detailed data, fractions of paddy and non-paddy irrigation, as well as the crop composition per month stay fixed (as obtained from MIRCA2000), while the total irrigated area per cell changes over time and is based on the FAOSTAT (FAO, 2012) reported irrigated areas. Irrigation water demand is computed using the FAO guidelines (Doorenbos and Pruit, 1977~~;~~, Allen et al., 1998): in case of non-paddy irrigation, water is applied whenever soil moisture falls below a pre-set value and then the soil column is replenished up to field capacity. In case of paddy irrigation, the water level is kept at a water depth of 5 cm above the surface until the late crop development stage (~ 20 days) before the harvest. After that, no irrigation is applied anymore such that the water level is allowed to drop to zero under infiltration and evaporation (Wada et al., 2014). The net irrigation demand is augmented to account for limited irrigation efficiency and losses. ~~In the standard parameterization of PCR-GLOBWB~~ In order t~~t~~o obtain irrigation water demand including losses, i.e. gross irrigation demand, net ~~the~~ irrigation water demand is multiplied with $(1 + f_i)$, with f_i a country-specific loss factor obtained from Rohwer et al. (2007).~~increased by 40% to obtain gross irrigation water demand (meaning an irrigation efficiency of (1/1.4)×100 = 71%.) However, it is possible to use spatio-temporal varying irrigation efficiencies if needed, which is the case for all other variables.~~

Non-irrigation water demand covers three sectors~~;~~, industry, households and livestock. For each of these sectors, the gross demand and net demand are prescribed to the model ~~and calculated using separate scripts~~. The calculation of net non-irrigation water demand, which varies with time, follows methods developed by Wada et al (2014). We refer to Wada et al. (2014) for an extensive description. Trends in water demand are prescribed on an annual basis as a function of population, electricity demand and gross domestic product (GDP) per capita. In addition, domestic water demand exhibits a seasonal variation on the basis of temperature. Domestic and industrial gross water demand is calculated from net water demand using a country-specific recycling ratio *RC* (based on development

stage or GDP per capita and additionally access to domestic water demand): gross = net/(1-*RC*). This takes into account that much of the domestic and industrial water is not consumed but returned as surface water. For livestock, the return flow is assumed to be zero, meaning all water is consumed.

Water withdrawal

The water withdrawal estimation is based on the work by de Graaf et al. (2014) and Wada et al. (2014). In PCR-GLOBWB 2 water withdrawal is set equal to gross water demand (summed over all the sectors) unless sufficient water is not available. In that case, water withdrawal is scaled down to the available water and then allocated proportionally to gross water demand per sector. Thus, no allocation preference is available in the standard parameterization of PCR-GLOBWB 2~~, but it would be rather straightforward to change this~~.

Water can be abstracted from three sources: surface water, groundwater (fossil and non-fossil) and desalinated water. The latter is prescribed (Wada et al., 2011a), while the fractions of the other two sources are determined as a function of their relative abundance. Groundwater and surface water availability are determined based on two-year running means of groundwater recharge and river discharge respectively, thus keeping track of the prevalence of local resources and their temporal change (de Graaf et al., 2014). These fractions determine on a monthly basis from which source water is abstracted. Surface water withdrawal is ceased if river discharge falls below 10% of the long-term average yearly discharge under naturalized flow conditions (determined by running the model without withdrawal). If, for some reason, the surface water amount is insufficient, the model falls back on groundwater to meet the resulting gap. Groundwater is first abstracted from the renewable groundwater storage, and if ~~not~~ this is not present, non-renewable groundwater is abstracted. The amount of groundwater that can be abstracted is, however, capped by the groundwater pumping capacity which is based on data by IGRAC GGIS database. The described dynamic allocation scheme is not always in line with local preferences or the infrastructure. However, there is a possibility to use ~~literature~~ fractions of groundwater and surface water withdrawal ~~withdrawal~~ reported in the literature~~and surface water withdrawal~~. For urban areas, we rely on the data set of McDonald et al. (2014) that states whether a surface water distribution infrastructure is available. If this is the case, industrial and domestic water withdrawals are mainly taken from surface water before abstracting groundwater. If surface water infrastructure is limited, groundwater source is prioritized (see e.g. Erkens and Sutanudjaja, 2015). For urban areas that are not in the McDonald (2014) data set, we give preference to the dynamic allocation scheme. For irrigation, we use the ratios supplied by Siebert et al. (2010) in regions where they are said to be reliable. In regions where they are not fully reliable, we take the average ratio provided by Siebert et al. (2010) and the one provided by the dynamic allocation scheme. For regions where the data of Siebert (2010) are not reliable (i.e., extrapolated data), we give preference to the dynamic allocation scheme.

Moreover, we cannot assume that all the water demand is supplied from surface water and groundwater resources in the same cell. Ideally, data about ~~the~~ local water redistribution networks and inter-basin transfers should be used to define ~~a~~ surface water and groundwater service areas. Unfortunately, this information is not available at the global scale. Therefore, in our current parameterization of PCR-GLOBWB 2, we pool water availability of desalinated and surface water over zones of approximately 1 arc-degree by 1 arc-degree ~~around each 5 arc-minute~~

~~cell~~size that are truncated by country ~~ and basin~~ borders if applicable. ~~Available surface water for abstraction is stored in channels, lakes and reservoirs within each cell and service area.~~For groundwater, 0.5 arc-degree zones are used. ~~Available surface water for abstraction is stored in channels, lakes and reservoirs within each cell and service area. Groundwater availability is also limited by the pumping capacity in the service area.~~

The downside of the current scheme is that a cell does not always have access to its nearest water resource if this lies outside its prescribed service area.

~~Available surface water for abstraction is stored in channels, lakes and reservoirs within each cell and service area. Groundwater availability is also limited by the pumping capacity in the service area.~~

Water consumption and return flows

In case of irrigation, all the withdrawn water is applied to the soil (non-paddy) or the water level on the field (paddy). Part of that water is lost by transpiration and part by soil and open water evaporation. Transpiration and evaporation together make up the irrigation water consumption. The remaining part of irrigated water is lost by percolation and contributes to groundwater recharge as return flow. Irrigation efficiency (not including conveyance losses) could also be calculated after the fact by the difference between withdrawal and transpiration. In case of domestic and industrial water use, water consumption depends on the recycling ratio RC and equals withdrawal×(1-RC), while withdrawal×RC constitutes return flow. All return flow is added to the surface water. For livestock, the consumption is set equal to the withdrawal and no return flow is assumed.

~~**2.4 Differences between PCR-GLOBWB 1 and 2**PCR-GLOBWB 2 has the following new capabilities compared to PCR-GLOBWB 1 (cf. Van Beek et al., 2011; Wada et al, 2011):the model was completely rewritten in PCRaster Python and now has a modular structure;the inputs and outputs are in the form of NetCDF files and output can be reported for daily monthly and yearly time steps;parameterizations are available at 30 arc-minute and 5 arc-minute resolution;water use (demand, withdrawal, consumption and return flow) is fully integrated;distinction is made between paddy and non-paddy irrigation and irrigation follows FAO guidelines;three different options for surface water routing are available and a surface water temperature module is fully integrated with the routing scheme;it is possible to run surface water routines separately with specific discharge from other sources (e.g. other land surface models);PCR-GLOBWB 2 can be coupled to a two-layer transient groundwater model (Sutanudjaja et al., 2014; De Graaf et al., 2017) and to the hydrodynamic models Delft3D Flexible Mesh (Kernkamp et al., 2011) or LISFLOOD-FP (Bates et al., 2010, see Hoch et al., 2017b).~~

22.45 Model code

The original PCR-GLOBWB version 1 (van Beek et al., 2011) was written in the PCRaster scripting language. PCRaster (Wesseling et al., 1996) is a high-level programming language that started as a dynamic raster-based Geographical Information System (GIS) and is tailored to spatiotemporal modelling for environmental and earth science applications. The generic nature of PCRaster with its many pre-existing ~~tailor-made~~ built-in hydrological functions and its syntax that reads like pseudo-code, generally results in concise ~~short and readable~~ model codes, short development times and limited programming errors. Karssenberg et al. (2010) developed a PCRaster Python package such that PCRaster functions, implemented in C++, can also be called via Python (http://www.python.org/). Using PCRaster Python ~~also~~ makes it possible for students and beginner modellers to contribute to the model quickly, while it allows experts to be more productive and focus on the science rather than on the programming language syntax. Realising the aforementioned advantages, PCR-GLOBWB, particularly starting from this version 2, has been rewritten in the Python scripting language.

To allow for exchanges of model components and, therefore, evaluate different model configurations, a component-based development approach (e.g Argent, 2004; Castronova and Goodall, 2010) was followed while developing the PCR-GLOBWB 2 model code. Each of the PCR-GLOBWB scientific modules described in section 2.3 is implemented in a separate Python class that needs to implement initialization and update methods. The latter designates changes of states and fluxes per time step. Each of module is initialized and executed by iteratively calling the update method via a main model script.

To run the model a so-called initialization file or configuration file is used (with extension .ini). In this file the following aspects are defined: the spatial and temporal domain, the time step, the settings of the different modules (e.g. which surface water routing, human water use or not etc.) and the locations and names of the parameter files and forcing files. ~~As mentioned above,~~ PCR-GLOBWB 2 uses NetCDF files for most input and all output, thus making it easier to exchange data with other scientists and use existing tools to analyse its output.

PCR-GLOBWB 2 generally runs best under Linux. ~~It is also possible to run it under Windows, but Windows memory constraints limit domain size and time steps simulated.~~ In order to run PCR-GLOBWB the following additional software needs to be installed: PCRaster version 4, Python versions 2.7 with Python packages numPy and netCDF4 and gdal version 1.8 or higher.

2.5 Differences between PCR-GLOBWB 1 and 2

PCR-GLOBWB 2 has the following new capabilities compared to PCR-GLOBWB 1 (cf. v~~V~~an Beek et al., 2011, Wada et al, 2011):

- the model was completely rewritten in PCRaster Python and now has a modular structure,
- the inputs and outputs are in the form of NetCDF files and output can be reported for daily monthly and yearly time steps,
- parameterizations are available at 30 arc-minute and 5 arc-minute resolutions,
- water use (demand, withdrawal, consumption and return flow) is fully integrated,
- distinction is made between paddy and non-paddy irrigation and irrigation follows FAO guidelines,
- three different options for surface water routing are available and a surface water temperature module is fully integrated with the routing scheme,
- it is possible to run surface water routines separately with specific discharge from other sources (e.g. other land surface models),
- PCR-GLOBWB 2 can be coupled to a two-layer transient groundwater model (Sutanudjaja et al., 2014, d~~D~~e Graaf et al., 2017) and to the hydrodynamic models Delft3D Flexible Mesh (Kernkamp et al., 2011) or LISFLOOD-FP (Bates et al., 2010, see Hoch et al., 2017b).

3. Model demonstration and evaluation

To test and evaluate the performance of PCR-GLOBWB 2~~of PCR-GLOBWB 2~~, we ran the model at both 30 arc-minute and 5 arc-minute resolution over the period 1958-2015. We compared the results of both simulations with discharge data from the ~~GRDC~~ Global Runoff Data Centre (GRDC, 2014), with total basin water storage estimates from GRACE (Gravity Recovery and Climate Experiment~~;~~, Wiese, 2015) and with water withdrawal data from the FAO AQUASTAT database (FAO, 2016).

3.1 Model run setup

3.1.1 Parameterization

We used the standard parameterization (parameters, forcing and their sources in Table A2) of PCR-GLOBWB 2 at 30 arc-minute and 5 arc-minute spatial resolutions to simulate global hydrology at daily resolution over 1958-2015. Outputs were reported as monthly averages. The parameterization was mostly unchanged from that given in v~~V~~an Beek and Bierkens (2009), but newer datasets were used if available, such as the GRAND (Lehner et al., 2011) dataset for reservoirs and MIRCA (Portmann et al., 2010) for crop areas. ~~Note that parameterizations were derived directly following their source data sets using hydrological concepts described in Van Beek and Bierkens (200~~ We stress that no calibration was performed. We ran the model with human water use options turned on and used the travel-time characteristic solution routing option.

3.1.2 Forcing

The forcing data set is based on time series of monthly precipitation, temperature and reference evaporation from the CRU TS 3.2 data set of Harris et al. (2014) downscaled to daily values with ERA40 (1958-1978~~;~~, Uppala et al., 2005) and ERA-Interim (1979-2015~~;~~ Dee et al., 2011). CRU is specified at 30 arc-minute spatial resolution and directly usable. We used ERA40 and ERA-I results that had been resampled by ECMWFs resampling scheme from their original resolutions (~1.2º and ~0.7º) to 30 arc-minutes first. Here, resampling means a form of spatial downscaling whereby the values of the larger ERA40 and ERA-I grid cells are assigned to the cell centers and then spatially interpolated onto ~~a~~ 30 arc-minute grids~~s grid using inverse distance interpolation~~." Precipitation was temporally downscaled by first applying a threshold of 0.1 mm/day to the ERA daily time series to estimate the number of rain days for ERA. The amount of rainfall below this threshold was proportionally allocated to the rain days. Next, the daily rainfall totals were scaled in order to reproduce the CRU monthly precipitation total using multiplicative scaling. Equally, monthly reference potential evaporation, computed with Penman-Monteith from the CRU data set, was scaled using multiplicative scaling and downscaled to daily data proportional to Hamon (1967) evaporation calculated from daily ERA temperatures. We elected not to calculate Penman-Monteith reference evaporation directly from the ERA40 and ERA-I data, in order to avoid the large calculation times needed to process the required meteorological values. For the air temperature, an additive scaling factor was used. To better simulate snow-dynamics for the 5 arc-minute model, the temperature values from CRU were further spatially downscaled to 5 arc-minutes using a temperature lapse-rate derived from the higher-resolution CRU ~~V1.0~~CL 2.0 climatology (New et al., 2002). For areas where the number of stations underlying the CRU data set was found to be small, preference was given to using directly the meteorological data from ERA. The method used to create the forcing data set is described more extensively in v~~V~~an Beek (2008).

3.1.3 Spin-up

The large groundwater response times for certain regions (e.g. Niger and Amazon) requires substantial spin-up for the groundwater volumes to be in equilibrium with the current climate. To reach this equilibrium, the model was spun-up using the average climatological forcing over the years 1958–2000 back-to-back for 150 years to reach a dynamic steady state. This spin-up was executed under naturalized condition which means no reservoirs and no human water use.

3.1.4 Computation time and parallelization

The models were run on Cartesius, the Dutch national supercomputer (https://userinfo.surfsara.nl/systems/cartesius). Without parallelization, the wall clock time for a one-year global simulation run of the 30 arc-minute model was about one hour. This entails that a one-year global simulation run with the 5 arc-minute model, might result in wall clock times of at least 36 hours. Hence, to speed-up computation, the 5 arc-minute model domain was divided into 53 groups of river basins such that it could be run as 53 separate processes. With this simple parallelization technique, the wall clock time for a one-year simulation run of the 5 arc-minute model reduced to about one hour again. Note that these computation times were obtained for simulations with the travel-time characteristic routing option. Calculation times would have been significantly longer if the kinematic wave routing had been used (e.g. about 6 hours for a one-year 5 arc-minutes global run including parallelization).

3.2 Data used for comparison

3.2.1 River discharge

We used discharge stations from GRDC (2014) to compare simulated discharge from PCR-GLOBWB 2 with monthly reported discharge. From all the globally available stations in the database, we selected a subset of stations using the following criteria: 1) allowing a not more than 15% difference in catchment area between PCR-GLOBWB 2 and the area reported with the GRDC discharge station~~;~~, 2) not more than 1 cell distance between the station location and the nearby location of a ~~main~~ river in PCR-GLOBWB 2~~;~~, 3) at least 1 year of discharge data. This yielded 5363 stations for the 5 arc-minute simulation, 3910 stations for the 30 arc-minute simulation and 3597 stations fulfilling the criteria for both resolutions. The minimum, median and maximum catchment sizes for the GRDC stations at the 5 arc-minute resolution are respectively 29, 2730 and $4.68 \cdot 10^6$km^2 and 31, 6560 and $4.68 \cdot 10^6$km^2 at the 30 arc-minute resolution. As we jointly compared the performance of both simulations, we used the set of 3597 locations throughout. The average time series length of these stations is equal to 36 years.

3.2.2 Total water storage

We compared total water storage (TWS) as simulated by PCR-GLOBWB 2 with the TWS estimated from GRACE (Gravity Recovery and Climate Experiment) gravity anomalies. We used the GRACE JPL Mascon product PL-RL05M (Wiese, 2015~~;~~, Watkins et al., 2015~~;~~, Wiese et al., 2016). Scanlon et al. (2016) suggest

that recent developments in mascon (mass concentration) solutions for GRACE have significantly increased the spatial localization and amplitude of recovered terrestrial TWS signals. They also claim that one of the advantages of using the mascon solutions relative to traditional SH (spherical harmonic) solutions is that it makes it much easier for non-geodesists to apply GRACE data to hydrologic problems. Note that although the data of PL-RL05M are represented on a 30 arc-minutes lat-lon grid, they represent the 3x3 arc-degree equal-area zones, which is the actual resolution of JPL-RL05M. We compared trends on a pixel-by-pixel basis. Given the coarse resolution of GRACE products of about 300 km by 300 km we compared correlations only for major river basins with an area of 900,000 km^2 and up.

3.2.3 Water withdrawal

The water withdrawal for a large number of countries is taken from FAO's AQUASTAT database (FAO, 2016). This data is on average reported in every 5 years. We compared simulated water withdrawal per sector and per water source (surface water and groundwater) with reported values per country and per reporting period, whenever available.

3.3 The global water balance simulated at 30 and 5 arc-minutes

We calculated the main global water balance components from the 30 arc-minute and 5 arc-minute simulations over the period 2000-2015. The results in Table 1 show that there are some differences between the two model runs, but values are in the same order of magnitude. The small difference in precipitation is due to the fact that the area of the land cells is slightly different at the two resolutions. Differences in evaporation and runoff show that the runoff and evaporation parameterization of PCR-GLOBWB 2 is not entirely scale-consistent. Differences in evaporation may also be causing the differences in irrigation water demand which in turn may explain the differences in water withdrawal. Recently, Samaniego et al. (2017) applied their multiscale parameter regionalization (~~MPR~~creating spatially variable parameter fields) technique (MPR) to PCR-GLOBWB 2 for the Rhine basin, showing that parameterizations that yield the same hydrological fluxes at different resolutions are possible~~scale-consistent flux-preserving parameterisation is possible~~. However, a global application of this method to all PCR-GLOWB 2 parameters is not possible yet. Nonetheless, when comparing the results of both model runs with data reported in the literature, it shows that the global water balance components are similar to recent

assessments (e.g. by Rodell et al., 2015) and groundwater withdrawal and total withdrawal estimates match those of previous studies (see Table 2).

From Table 1, it can also be seen that there is a negative change in total terrestrial water storage in both model runs. Table 1 shows that this can only be partly explained by groundwater depletion, which is localized to certain regions (see also Sect. 3.4.2). Further analysis shows that this change can also be attributed to the trends in precipitation forcing used, particularly over the tropics.

Table 1. Global Water balance components and human water withdrawal (in km^3/year and mm/year) over the period 2000-2015 as obtained from the 30 arc-minutes and the 5 arc-minute simulations. The numbers are shown to high significance to show the water balance closure. This does not mean that we pretend to know e.g. global discharge with a km^3 accuracy (actual accuracy of the large fluxes is more in the order of 10^3 km^3)

		30 arc-min		5 arc-min	
		km^3/year	mm/year	km^3/year	mm/year
Global water balance	Precipitation	107452	808	107495	811
	Desalinated water use	3	0.02	2	0.01
	Runoff	42393	319	43978	332
	Evaporation*	65754	494	63974	483
	Change in total water storage	-693	-5	-455	-3
Groundwater budget	Groundwater recharge	27756	209	25521	193
	Groundwater withdrawal	737	6	632	5
	Non-renewable groundwater withdrawal (groundwater depletion)	173	1	171	1
	Renewable groundwater withdrawal	564	4	460	3
Withdrawal by sector	Agricultural water withdrawal (irrigation + livestock)	2735	21	2309	17
	Domestic water withdrawal	380	3	314	2
	Industrial water withdrawal	798	6	707	5
Withdrawal by source	Total water withdrawal	3912	29	3330	25
	Surface water withdrawal	3172	24	2697	20
	Desalinated water use	3	0.02	2	0.01
	Groundwater withdrawal	737	6	632	5

* Includes consumptive water use for livestock, domestic and industrial sectors

		30 arc-min (km^3/year)	5 arc-min (km^3/year)
Global water balance	Precipitation	107452	107495
	Desalinated water use	3	2
	Runoff	42393	43978
	Evaporation*	65754	63974
	Change in total water storage	-693	-455
Groundwater budget	Groundwater recharge	27756	25521
	Groundwater withdrawal	737	632
	Non-renewable groundwater withdrawal (groundwater depletion)	173	171
	Renewable groundwater withdrawal	564	460
Withdrawal by sector	Agricultural water withdrawal (irrigation + livestock)	2735	2309
	Domestic water withdrawal	380	314
	Industrial water withdrawal	798	707
Withdrawal by source	Total water withdrawal	3912	3330
	Surface water withdrawal	3172	2697
	Desalinated water use	3	2
	Groundwater withdrawal	737	632

* Includes consumptive water use for livestock, domestic and industrial sectors

Table 2. Groundwater withdrawal ~~(a)~~ and total water withdrawal ~~(b)~~ as compared to other studies (in km^3/year)

	Source	Year	Value (km^3/year)
Groundwater withdrawal	Wada et al. (2010) (from the IGRAC database)	2000	734 (±87)
	Döll et al. (2012)	1998-2002	571
	Döll et al. (2014) (their Table 2).	2003-2009	690-888
	Döll et al. (2014) (their Table 6).	2000-2009	665
	Pokhrel et al. (2015)	1998-2002	570 (±61)
	Hanasaki et al. (2018)	2000	789 (±30)
	This study (5 arc-minutes)	2000-2015	632
Total water withdrawal	Vörösmarty et al. (2005)	1995-2000	3560
	Oki and Kanae (2006)	contemporary	3800
	Döll et al. (2012)	1998-2002	4340
	Döll et al. (2014) (their Table 2)	2003-2009	3000-3700
	FAO (2016)	2010	3583
	Hanasaki et al. (2018)	2000	3628 (±75)
	This study (5 arc-minutes)	2000-2015	3330

a) Groundwater withdrawal

Source	Year	Value (km^3/year)
Wada et al. (2010) (from the IGRAC database)	2000	734 (±87)
Döll et al. (2012)	1998-2002	571
Döll et al. (2014) (their Table 2).	2003-2009	690-888
Döll et al. (2014) (their Table 6).	2000-2009	665
Pokhrel et al. (2015)	1998-2002	570 (±61)
Hanasaki et al. (2018)	2000	789 (±30)
This study (5 arc-minutes)	2000-2015	632

b) Total water withdrawal

Source	Year	Value (km^3/year)
Vörösmarty et al. (2005)	1995-2000	3560
Oki and Kanae (2006)	2006	3800
Döll et al. (2012)	1998-2002	4340
Döll et al. (2014) (their Table 2)	2003-2009	3000-3700
FAO (2016)	2010	3583
Hanasaki et al. (2018)	2000	3628 (±75)
This study (5 arc-minutes)	2000-2015	3330

3.4 Evaluation of the 30 and 5 arc-minute simulations

3.4.1 Discharge

When evaluating the simulated discharge with discharge observations from GRDC, we used the monthly values and calculated three different measures~~: 1)~~. The first one is the correlation coefficient between monthly simulated and observed GRDC time series, which is a measure of reproducing correct timing of high and low discharge. A correlation coefficient of 1 indicates~~s~~ perfect timing.~~;~~ ~~2)~~The second measure is the Kling-Gupta efficiency coefficient or KGE (Gupta et al., 2009) which equally measures bias, differences in amplitude and differences in timing between monthly simulated and observed GRDC time series. The KGE varies between 1 and minus infinity, where 1 means a perfect fit in terms of bias, amplitude and timing. ~~;, 3)~~ The last metric is the anomaly correlation, i.e. the correlation between monthly time series after the seasonal signal (climatology) has been removed. This statistic measures the ability of the model to correctly simulate timing of seasonal and the inter-annual anomalies from the yearly climatology. ~~-~~This is to test if the model is able to capture the monthly scale and inter-annual anomalies in discharge (i.e. on the monthly scale) when the dominant seasonal trend is removed from observations and simulations. ~~It shows if the model is capable of capturing hydrological extremes and is not only driven by the climatology.~~ An anomaly correlation of 1 indicates perfect characterization of ~~the~~inter-annual anomalies ~~extremes~~ and values below 0 indicate~~s~~ a lack thereof.

Figure 2~~3~~ shows maps of the correlation coefficients for the GRDC stations considered and Figure 3~~4~~ shows histograms of correlation and KGE values. Both figures show that the ~~validation~~ evaluation results of the 5 arc-minute simulation are ~~notably~~ generally better than those of the 30 arc-minute simulation. For the 30 arc-minute model, the number of catchments with KGE > 0, 0.3 and 0.6 are equal to 48%, 26% and 7% of the total catchments respectively. For the 5 arc-minute model, these values are respectively equal to 63%, 40% and 12% of the total catchments. Note that for both runs the standard parameterization was used. Possible explanations for the better performance of the 5 arc-minute run are: a better delineation of the ~~outline~~ ~~shapes~~shape of the basins, particularly the smaller ones, a better characterization of basin relief and the drainage network, more accurate sub-grid parameterization of soil and land cover due to a smaller scale-gap that needs to be overcome, better estimates of the basin storage and better snow dynamics due to the downscaling of temperature to 5 arc-minute resolution. The KGE values are less favourable than the correlation coefficients. This is mostly due to biases in runoff caused by ~~to~~ incorrect meteorological forcing.

It is difficult to exactly assess which of these factors are most important in determining the improvement. Inspecting the histograms of correlation and KGE (Figure 4~~3~~) shows that the improvement is mostly apparent for the smaller sized catchments, which supports the notion that a better delineation of the catchments' shape, topography and drainage network could be the cause. However, ~~-~~disentangling these individual effects would require further study. To investigate the possible effects of better snow dynamics we classified the GRDC stations into stations below 1000 m altitude (above mean sea-level) and those above 1000 m. The GRDC stations above 1000 m are expected to experience precipitation falling as snow during periods of the year. The r~~R~~esults in Figure 5~~4~~ clearly show that the improvement is larger for the higher GRDC stations, This supports the explanation that better snow dynamics due to temperature lapsing in combination with a better resolved digital elevation model is partly responsible for the superior~~better~~ results at 5 arc-minutes. We also investigated if improvements were notably different between climate zones, by separately calculating KGEs for GRDC stations in the Köppen-Geiger zones A (Tropical), B (Desert), C (Temperate) and D (Continental). The results (not shown) show that the improvement is equally visible for climate zones A, B and C ~~-~~and less so for D (continental). Without further analysis this is difficult to explain. Note however that the continental climate zone is somewhat under-represented in the GRDC dataset due to the low measurement densities over Russia, although it is well represented in the U.S. So, it may be that the global improvements shown in Figure 4~~3~~ are somewhat positively biased.

~~The KGE values are less favourable than the correlation coefficients. This is mostly due to biases in runoff caused by to incorrect meteorological forcing.~~

The maps of correlations (Figure 2) show the best results in Europe and North America where the meteorological forcing is generally more accurate as a result of more data used in the re-analysis products

and higher station availability in the CRU data set. Also, monsoon-dominated basins are well simulated due to the strong seasonal nature of both forcing and related discharge. The improvement of the 5 arc-minute simulation over the 30 arc-minute simulation in Europe is mostly seen in the Alps and the Norwegian mountains. This reflects the fact that topography and thus snow dynamics is better represented at higher resolution as shown in Figure 4. The least accurate results are obtained for some of the African rivers, in particular the Niger where the groundwater recession coefficients are probably over-estimated and inland delta evaporation is under-estimated, for some rivers in the Rocky Mountains, which may be the result of errors in snow dynamics and for continental Eastern Europe, which is most likely explained by an over-estimation of the groundwater recession constants.

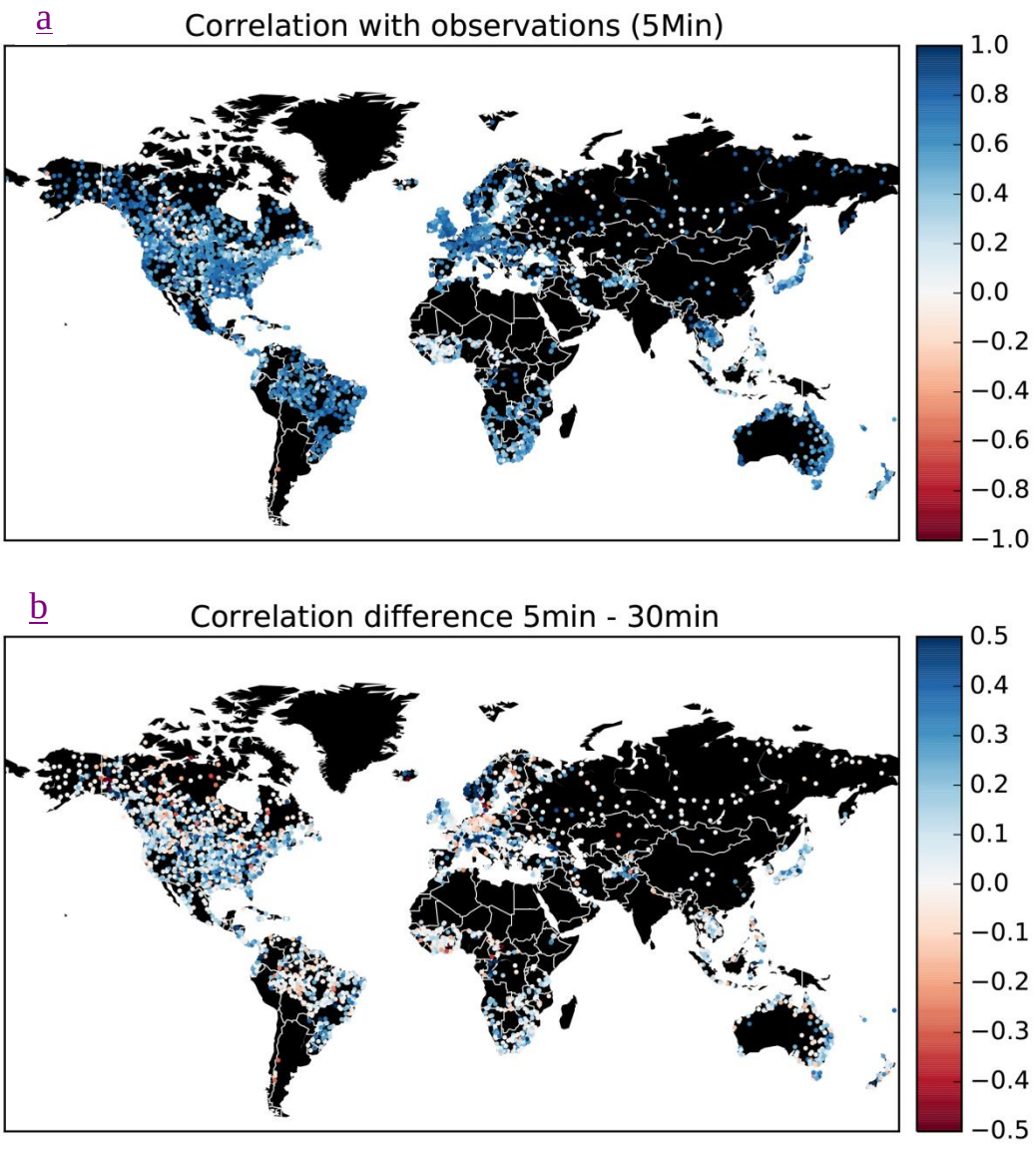

Figure 2~~3~~. Maps of correlation between simulated and observed discharge time series for 3597 GRDC discharge stations; a. results for the 5 arc-minutes simulation; b. difference between results for 5 arc-minutes and 30 arc-minutes simulation.

~~The maps of correlations (Figure 3) show the best results in Europe and North America where the meteorological forcing is generally more accurate as a result of more data used in the re-analysis products and higher station availability in the CRU data set. Also, monsoon-dominated basins are well simulated due to the strong seasonal nature of both forcing and related discharge. The improvement of the 5 arc-minute simulation over the 30 arc-minute simulation in Europe is mostly seen in the Alps and the Norwegian mountains. This reflects the fact that topography and thus snow dynamics is better represented at higher resolution as shown in Figure 5. The least accurate results are obtained for some of the African rivers, in particular the Niger where the groundwater recession coefficientsconstants are probably over-estimated and inland delta evaporation is under-estimated, and for some rivers in the Rocky Mountains, which may be the result of errors in snow dynamics and for continental Eastern Europe, which is most likely explained by an over-estimation of the groundwater recession constants.. Although results are generally better, the spatial distribution of results is similar to those found by Van Beek et al. (2011) for PCR-GLOBWB 1. The histograms of validation results in Figure 4 do not show a strong relationship between catchment size and validation statistics. This suggests that the improvements of model results equally apply to all catchment sizes when moving from a coarser to higher resolution.~~

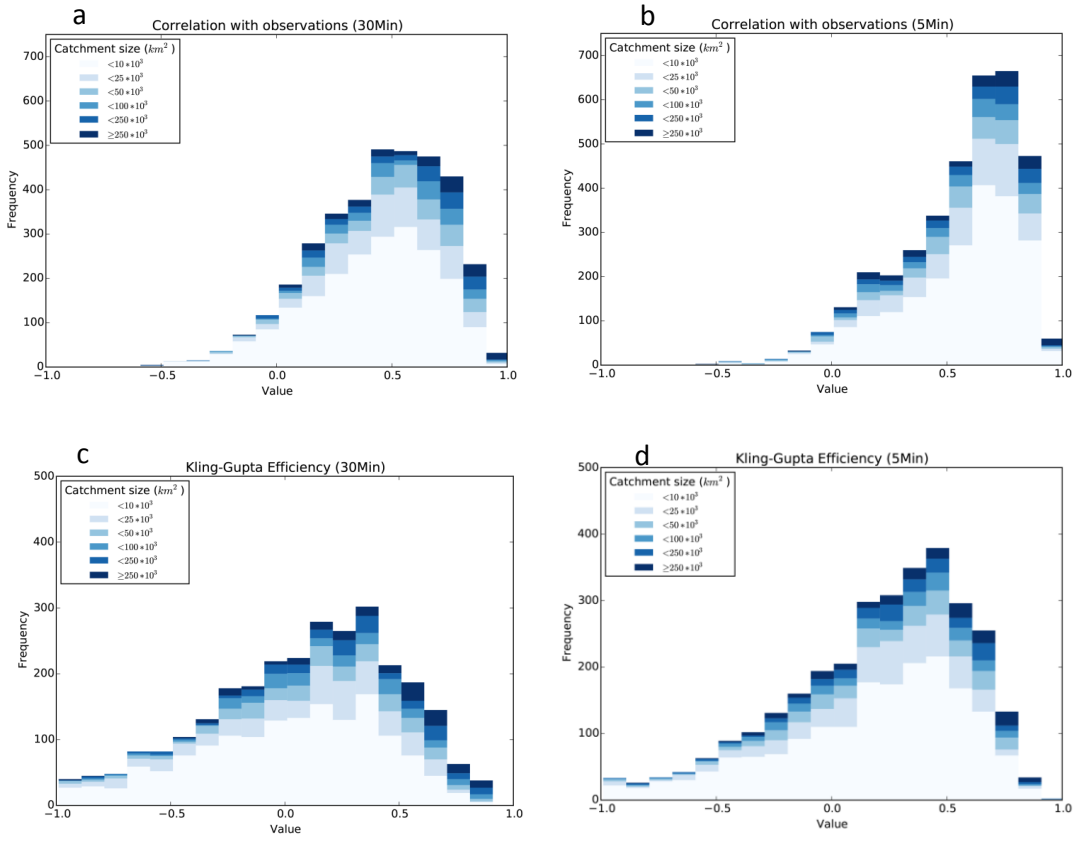

Figure ~~4~~3. Histograms of ~~validation~~ evaluation statistics showing the correlation and Kling-Gupta efficiency (KGE) values for the simulated discharge for the 30 arc-minutes and the 5 arc-minute simulations based on 3597 GRDC discharge stations~~;~~, a. correlation 30 arc-minute simulation~~;~~, b. correlation 5 arc-minute simulation~~;~~, c. KGE 30 arc-minute simulation~~;~~, d. KGE 5 arc-minute simulation~~;~~, note: the percentage catchments with KGE < -1 are 21% and 12% for 30 and 5 arc-minutes respectively.

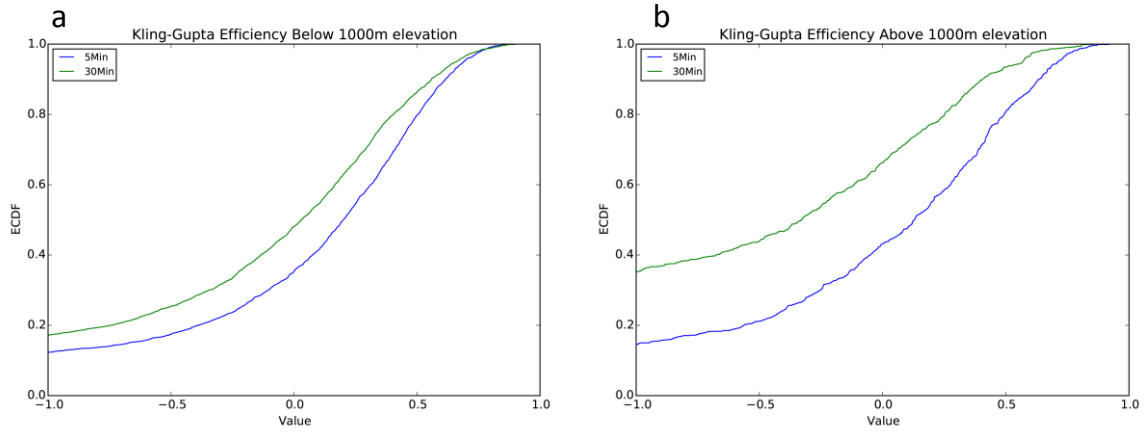

Figure ~~5~~4. Cumulative frequency distributions of Kling-Gupta efficiency (KGE) values for GRDC stations that are positioned below (a) and above (b) 1000 m a.m.s.l. It can be expected that for the stations above 1000 m, the upstream area is influenced by snow dynamics.

The histograms of the anomaly correlation are shown in Figure ~~5~~65. The anomaly correlations are generally lower than the correlations, showing that seasonality explains part of the skill in many regions where seasonal variation is dominant when compared to intra-annual or inter-annual variability. Clearly, the 5 arc-minute results are much better than those of the half-degree simulation, indicating a higher skill with regard to capturing inter-annual ~~extremes and~~ anomalies. Figure 6 shows a map of the difference between the anomaly correlation and the correlation for the 5 arc-minute case. This map shows that there are some regions where the anomaly correlation is better than the correlation (blue colours), e.g. snow-dominated regions in Canada and the Niger basin. These are catchments where the model has difficulty reproducing the correct seasonality as a result of errors in snow dynamics (Canada) or groundwater dynamics (Niger). Also, in case of the Niger River, not representing the inner delta flooding and resulting high evaporation may be the cause of poor seasonal timing of discharge.

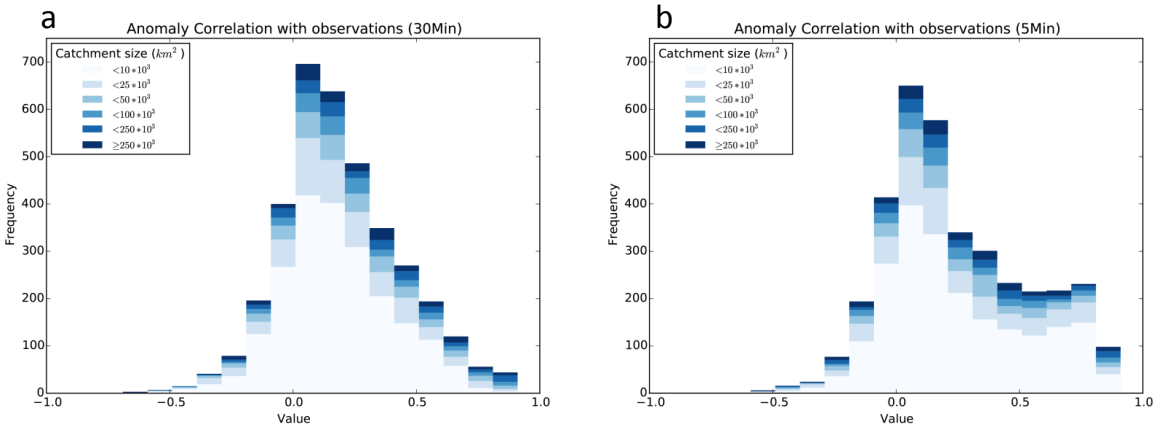

Figure ~~6~~5. Histograms of ~~validation~~ evaluation statistics showing the anomaly correlation for the simulated discharge for the 30 arc-minutes and the 5 arc-minute simulations based on 3597 GRDC discharge stations~~;~~, a. anomaly correlation half arc-degree simulation~~;~~ b. anomaly correlation 5 arc-minute simulation.

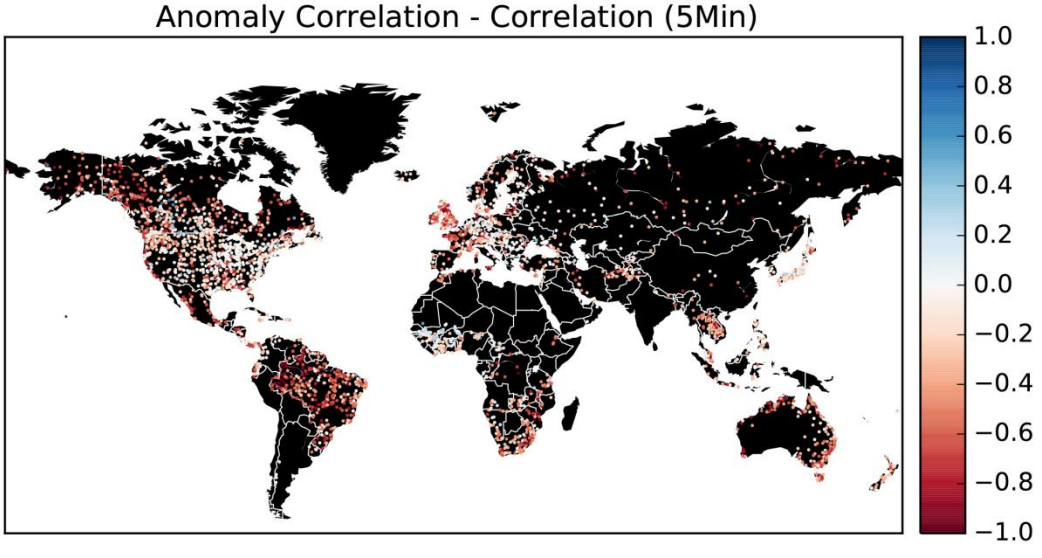

Figure ~~7~~6. Map showing for the 5 arc-minute~~s~~ run the difference between the correlation and the anomaly correlation between simulated and observed discharge time series for 3597 GRDC discharge stations~~;~~ negative values mean that the correlation is higher than the anomaly correlation.

3.4.2 Total water storage

Figure ~~7~~ ~~8~~7 compares the trends in 5 arc-minute simulated total water storage (TWS) with those from GRACE, estimated as the average change in m/year over the period 2003-2015. Generally, the PCR-GLOBWB 2 simulation is able to capture major groundwater depleted regions as suggested by GRACE, such as those in the Central Valley aquifer~~-~~, the High Plains aquifer, the North China Plain aquifer, as well as parts of the Middle East, Pakistan and India. For these regions, the absolute rates of TWS change (i.e. TWS declines) of PCR-GLOBWB 2 are generally larger, while the spatial pattern in the GRACE map tends to be smoother. This is mainly due to the lower resolution and spatial averaging used in the GRACE product, as well as the fact that the current PCR-GLOBWB 2 simulation does not include lateral groundwater flow between cells. In the polar regions where GRACE estimates mass loss due to melting glaciers and ice sheets, PCR-GLOBWB 2 simulates accumulation as a result of lack of a glacier parameterization. Finally, there are some clear differences over the Amazon and some parts of Africa. A possible explanation are errors in meteorological forcing data, which is not very accurate in these parts, but also problems with the over-estimation of PCR-GLOBWB's groundwater response times in these regions which therefore fail to be sufficiently sensitive to recent changes in terrestrial precipitation.

Further analyses were conducted at the basin-scale resolution, where both TWS time series of PCR-GLOBWB 2 and GRACE *JPL-RL05M* were averaged over a river basins areas map derived from the 5 arc-minute PCR-GLOBWB drainage network. We identified all river basins with sizes larger than 900,000 km^2, which is similar to the GRACE resolution. Smaller river basins were merged to the nearest river basins or grouped together. For the remaining map of large basins, the correlations between PCR-GLOBWB 2 and GRACE basin-average monthly and annual TWS time series were calculated. Monthly correlation provides information about PCR-GLOBWB's ability to correctly time TWS seasonal variability (with a value equal to 1 for perfect timing), while the correlation for annual time series measures inter-annual variability.

The results in Figure ~~8~~ ~~9~~8 show that PCR-GLOBWB 2 is able to capture GRACE's TWS seasonality for most basins around the world, with the exception of some cold regions in high latitudes (e.g. the Yukon River basin, Iceland). This shortcoming is most likely due to the lack of a proper representation of glacier and ice processes in PCR-GLOBWB 2. As expected, the correlation values for inter-annual time series are generally lower than the ones for monthly time series. There are some areas with negative correlation values, such as the Amazon, Niger and Nile river basins. Apart from the uncertainty in the GRACE signal, these deficiencies may be related to errors in model forcing and structural errors such as errors in the groundwater response time and the effects of wetlands that have not been represented sufficiently well.

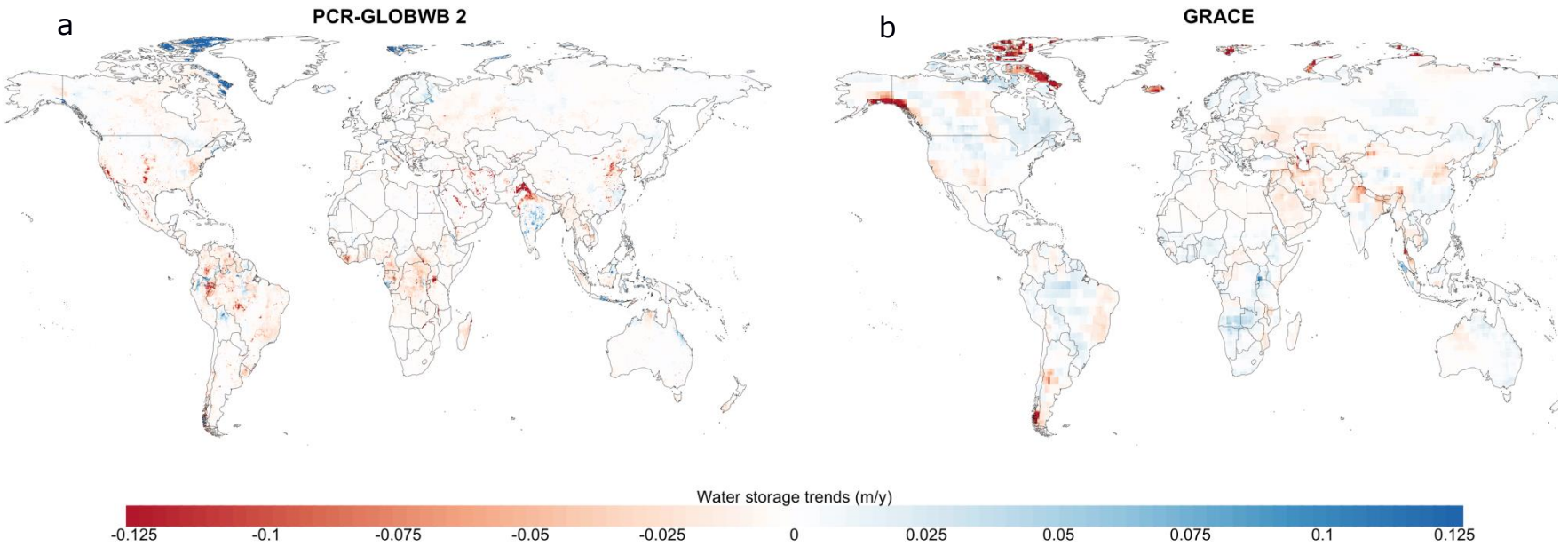

Figure ~~8~~7. Comparison of PCR-GLOBWB 2 total water storage trends (m/year) with those estimated with GRACE over the period 2003-2015. a. TWS trends simulated with PCR-GLOBWB at 5 arc-minutes resolution (~10 km at the equator). Negative values indicate declining TWS (e.g. groundwater depleted regions). b. TWS trends obtained based on the GRACE JPL PL-RL05M Mascon product. The GRACE data were resampled to the resolution of 30 arc-minutes, but they actually represent the 3 x 3 arc-degree (~300 km x 300 km) area, which is the native resolution of the GRACE signal.

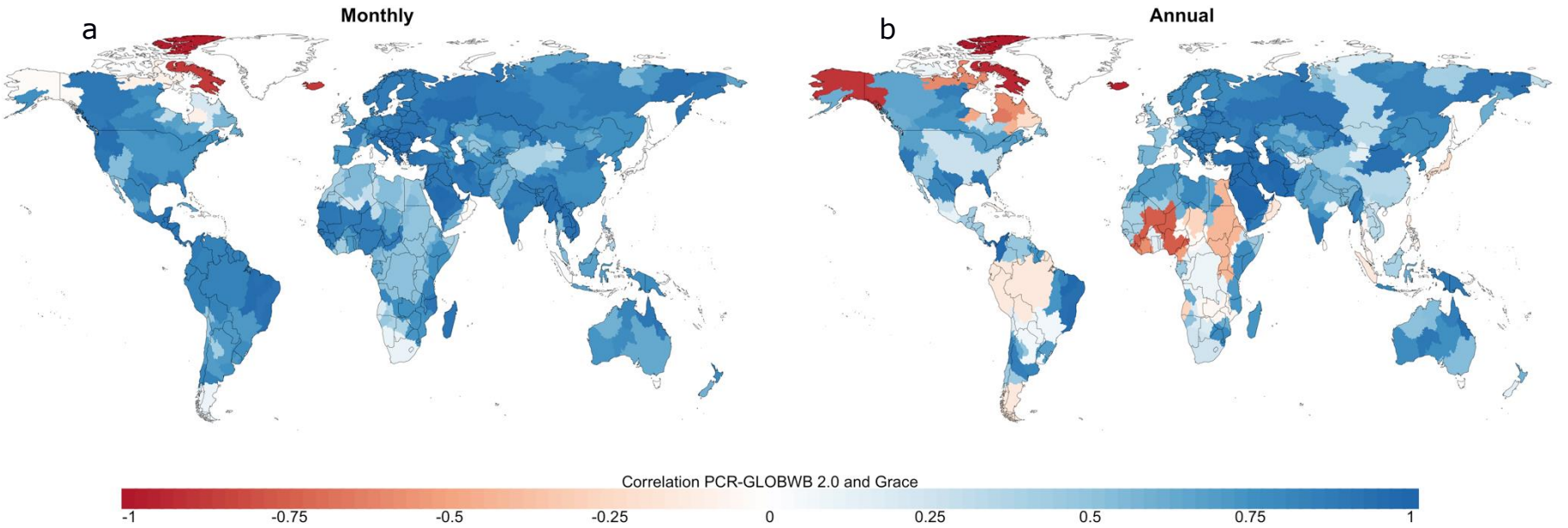

Figure ~~9~~8. a. Correlation between monthly TWS time series simulated PCR-GLOBWB 2 and the GRACE JPL PL-RL05M Mascon product over the period 2003-2015. b. Comparison of annual TWS series (inter-annual variability). Comparison is only done for the larger basins over 900,000 km2, conform the 3x3 arc-degree resolution of GRACE.

874

a) Country total withdrawal (km^3/year) in 1968-1992

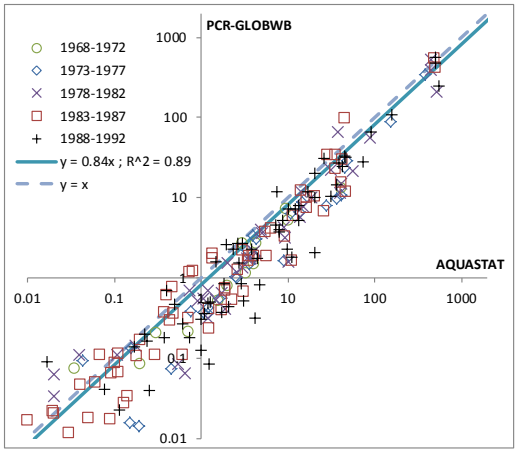

b) Country total withdrawal (km^3/year) in 1993-2015

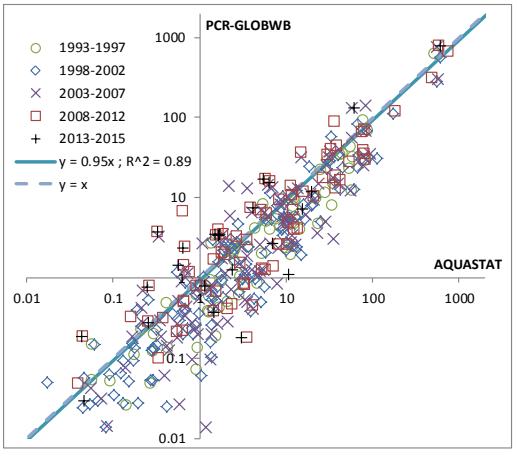

c) Country groundwater withdrawal (km^3/year) in 1968-1992

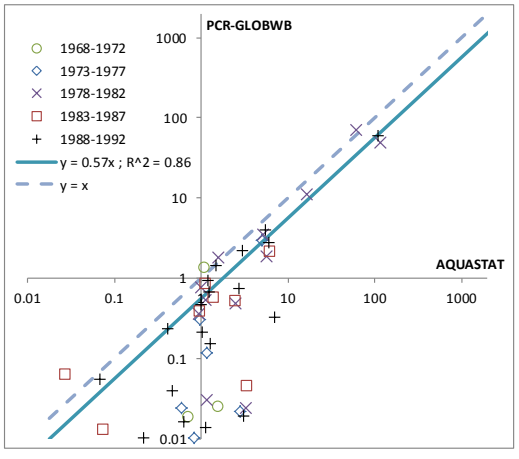

d) Country groundwater withdrawal (km^3/year) in 1993-2015

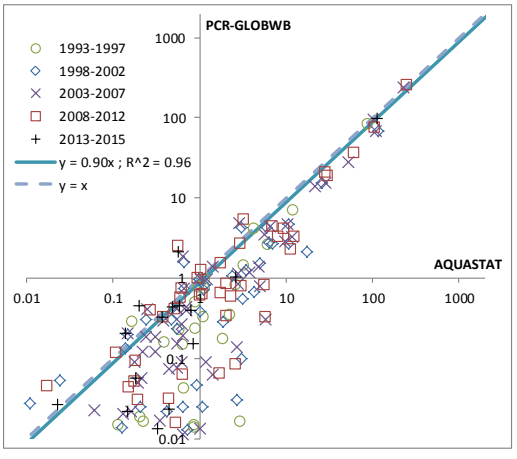

e) Country surface water withdrawal (km^3/year) in 1968-1992

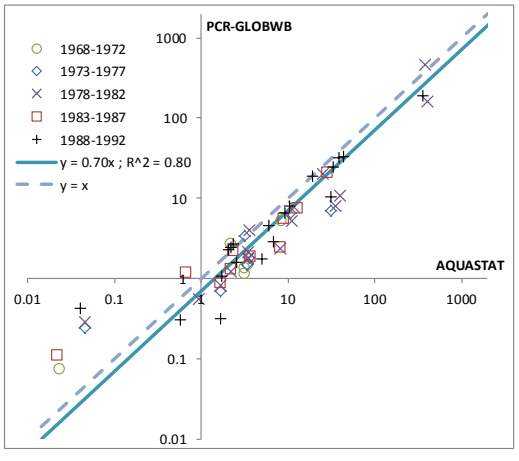

f) Country surface water withdrawal (km^3/year) in 1993-2015

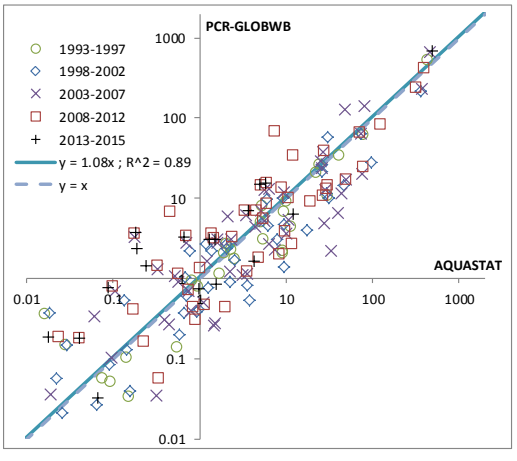

875

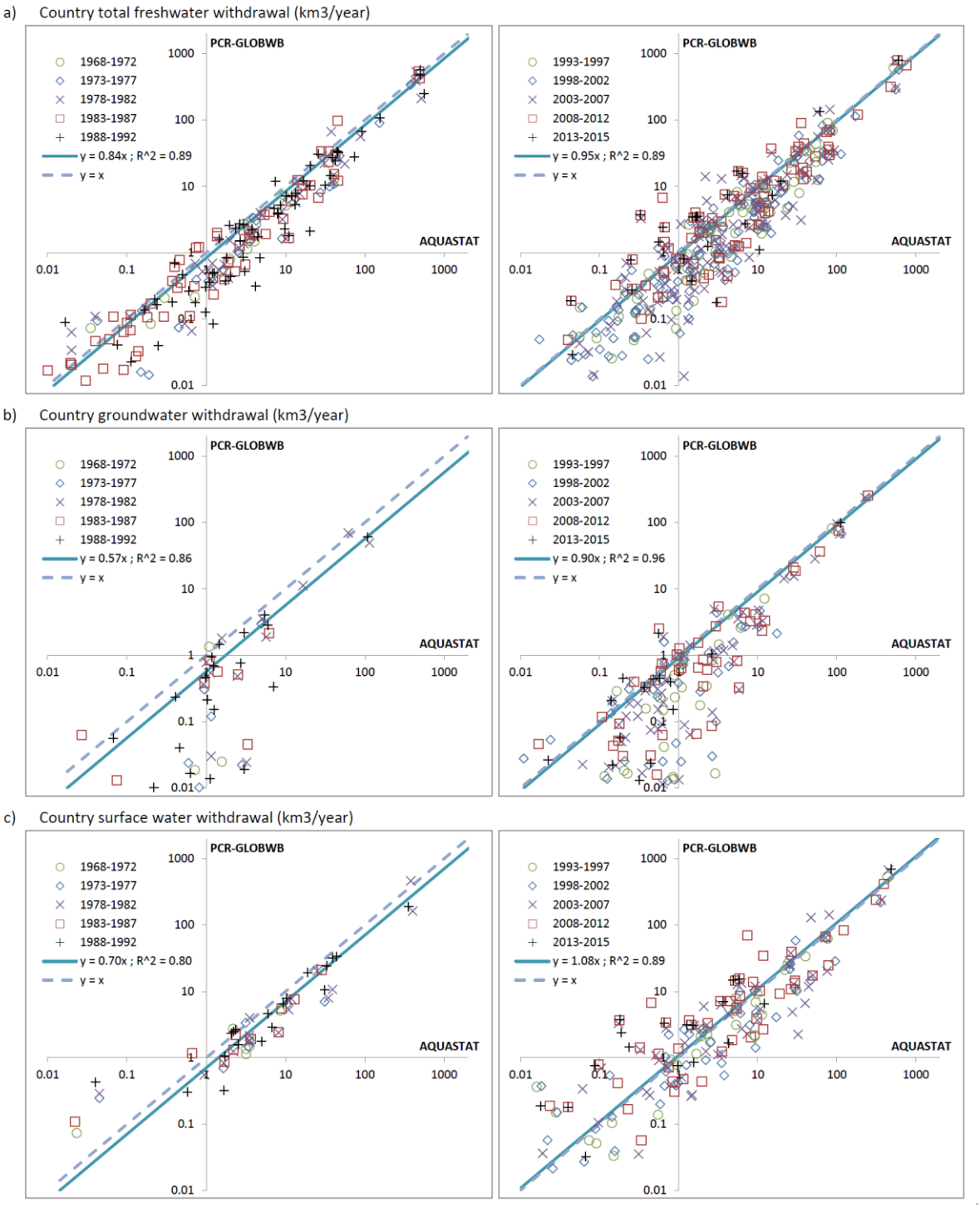

Fig. ~~10~~9: Country water withdrawal (km^3/year) by source~~:~~, ~~validation~~ evaluation of simulations with PCR-GLOBWB 2 with reported values in AQUASTAT (FAO, 2016)~~ for various periods~~. The scatterplots on the left (a, c, e) are for the period 1968-1992, while the right ones (b, d, f) are 1993-2015. The uppermost plots (a, b) are for ~~:, a)~~ total water withdrawal~~:, b)~~the middle ones (c, d) are groundwater withdrawal~~:, c)~~and the

lowermost charts (e, f) are surface water withdrawal~~:~~. ~~r~~Regression coefficient based on regression to non-log transformed data with intercept kept zero.~~,~~

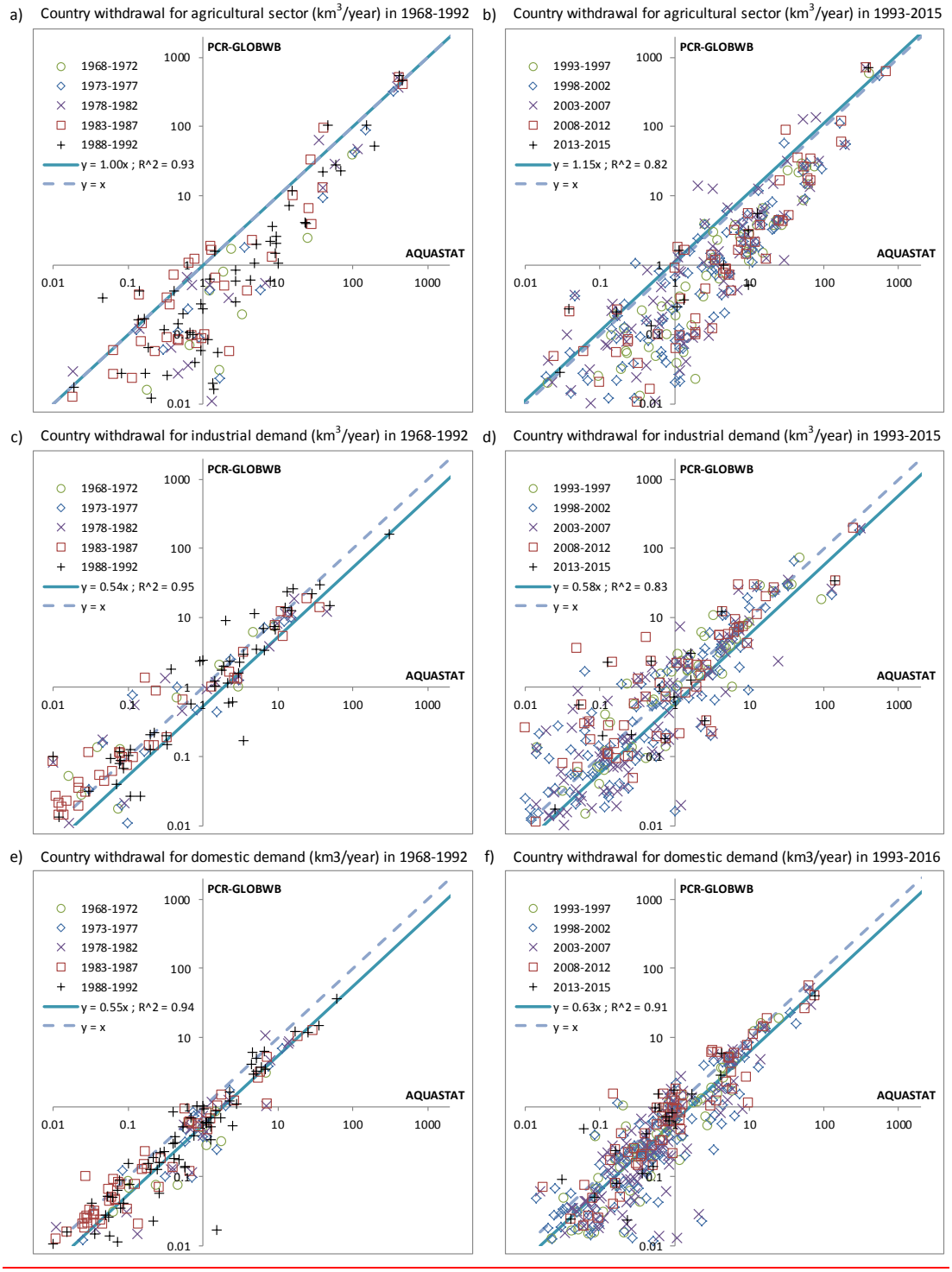

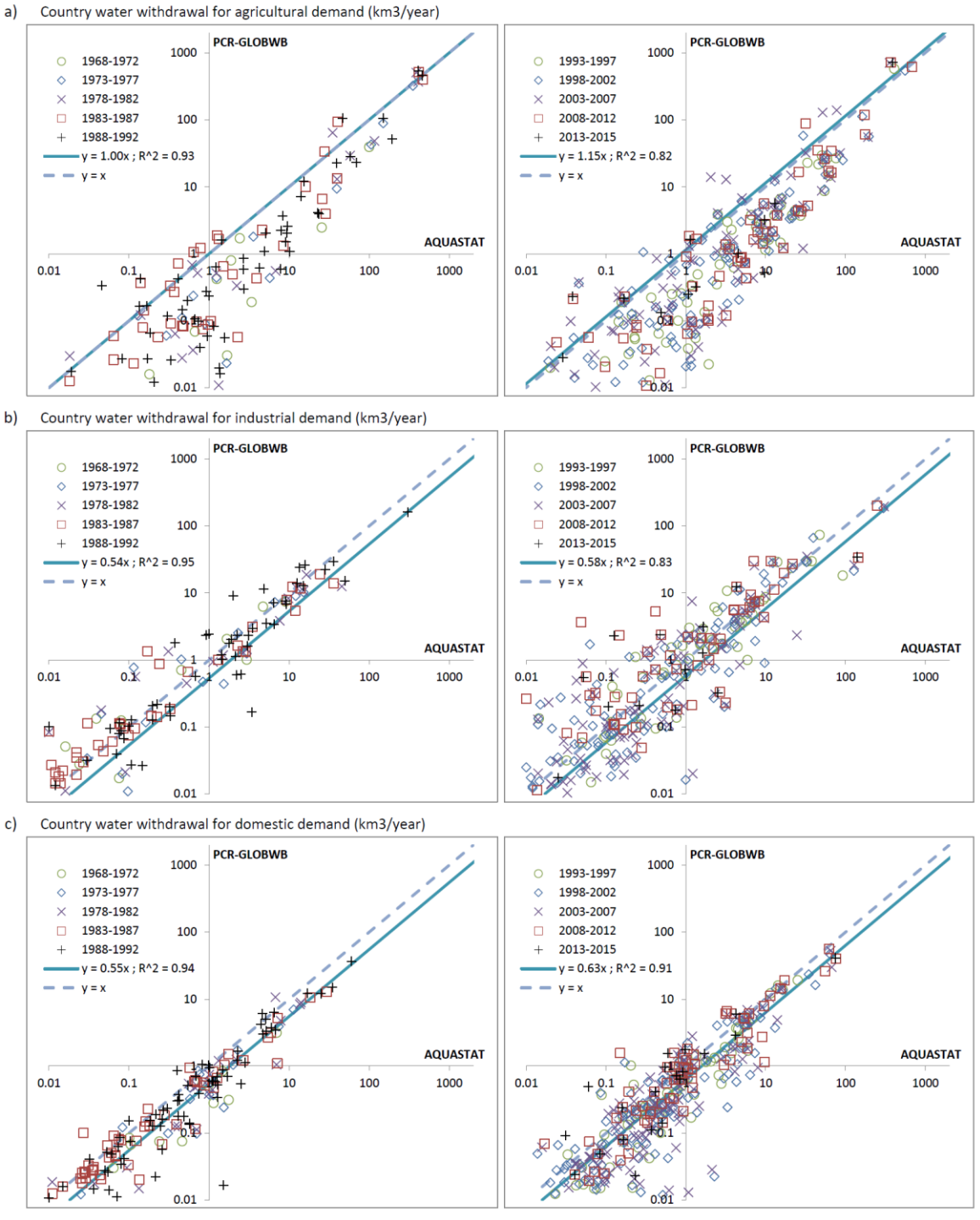

Fig. 10: Country water withdrawal (km3/year) by sector, evaluation of simulations with PCR-GLOBWB 2 with reported values in AQUASTAT (FAO, 2016). The scatterplots on the left (a, c, e) are for the period 1968-1992, while the right ones (b, d, f) are 1993-2015. The uppermost plots (a, b) are for withdrawal for agricultural purpose, the middle ones (c, d) are industrial withdrawal, and the lowermost charts (e, f) are domestic. Regression coefficient based on regression to non-log transformed data with intercept kept zero.

~~*Fig. 11: Country water withdrawal (km^3/year) by sector;₁ validation of simulations with PCR-GLOBWB 2 with reported values in AQUASTAT (FAO, 2016) for various periods;₁ a) withdrawal for agricultural demand (irrigation and livestock);₂ b) withdrawal for industrial demand;₂ c) withdrawal for domestic demand. regression coefficient based on regression to non-logtransformed data with intercept kept zero.*~~

3.4.3 Water withdrawal

We compared simulated water withdrawal data from PCR-GLOBWB 2 with reported withdrawal data per country from AQUASTAT (FAO, 2016). The results are shown subdivided per source (Figure ~~9~~109) and per sector (Figure 1~~10~~0).-. Total water withdrawal and surface water withdrawal ~~are simulated~~are simulated reasonably well (R^2 between 0.84 and 0.96 and regression slopes between 0.70 and 1.08). However, groundwater withdrawal is underestimated for the smaller water users. A likely explanation for this is occasional groundwater withdrawal by farmers during dry periods- in- areas that have not been mapped as irrigated crops in MIRCA, such as grasslands in e.g. Germany and the Netherlands, while ~~this groundwater~~this groundwater withdrawal is reported in AQUASTAT.

When looking at water withdrawal per sector, results are mixed. The largest agricultural water users are well captured, but the smaller ones are clearly underestimated. This is related to the fact that in many regions of the smaller water use countries, water is used for irrigation only occasionally during dry summers, while these areas are not mapped as irrigated crops in MIRCA. Also, many of these countries use irrigation technology that is not part of MIRCA, e.g. subsurface drainage by artificially high surface water levels such as in a number developed delta regions in the world. However, even though these smaller countries are not well represented, PCR-GLOBWB 2 is still able to capture the big water users, which have a significant impact on the water cycle and are most important for global scale analyses.

Both industrial and domestic water ~~withdrawal are~~withdrawals are underestimated. The underestimation of industrial water withdrawal is partly caused by the fact that we do not include water withdrawal for thermo-electric cooling of power plants. The underestimation of domestic water withdrawal comes from the fact that we assume that the priority of water allocation is proportional to demand. This means that in times of shortage, water withdrawal is reduced with an equal percentage for agriculture, industry and domestic use. In many countries however, there is a priority series, whereby domestic demand is first met, industrial demand next and agricultural demand comes last. As a result, we underestimate domestic water withdrawal and it also partly causes the underestimation of industrial water withdrawal. This is corroborated by plotting gross water demand (which would be withdrawal if no shortage would occur) against AQUASTAT data. These plots (not shown here) result in a regression slopes of 0.~~88~~68-0.~~96~~75 for industrial demand and 0.~~94~~78-0.9~~7~~2 for domestic demand. These results thus reveal that the water allocation scheme of PCR-GLOBWB 2 should be further improved.

~~These figures show that PCR-GLOBWB 2 is able to reproduce reported withdrawal values reasonably well (R^2 between 0.80 and 0.96 and regression slopes between 0.54 and 1.15). There is some underestimation of groundwater withdrawal for the countries with lower withdrawal values. This may be the result of not sufficiently accounting for domestic groundwater withdrawal in populated areas. Also, Figure 10 shows that agricultural water withdrawal is underestimated for countries with smaller withdrawal. A possible cause of this may be the overestimation of irrigation efficiency.~~

4. Conclusions and future work

We presented the most recent version of the open source global hydrology and water resources model PCR-GLOBWB. This version, PCR-GLOBWB 2, has a global coverage at 5 arc-minute resolution. Apart from the higher resolution, the new model has an integrated water use scheme, i.e. every day sector specific water demand is calculated, resulting in groundwater and surface water withdrawal, water consumption and return flows. Dams and reservoirs from the GranD database (Lehner et al., 2011) are added progressively according to their year of construction. PCR-GLOBWB 2 has been rewritten in Python and uses PCRaster-Python functions (Karssenberg et al., 2007). It has a modular structure, which makes the replacement and maintenance of model parts easier. PCR-GLOBWB 2 can be dynamically coupled to a global 2-layer groundwater model (dDe Graaf et al., 2017; Sutanudjaja et al., 2014; Sutanudjaja et al., 2011) and a one-way coupling to hydrodynamic models for large-scale inundation modelling (Hoch et al., 2017b) is also available.

Comparing the 5 arc-minute with 30 arc-minute simulations using discharge data we clearly find an improvement in the model performance of the higher resolution model. We find a general increase in correlation, anomaly correlation and KGE, indicating that the higher resolution model is better able to capture the seasonality, hydrological extremesinter-annual anomalies and the general discharge characteristics. Also, PCR-GLOBWB 2 is able to reproduce trends and seasonality in total water storage as observed by GRACE for most river basins. It simulates the hotspots of groundwater decline that around in GRACE as well. Simulated total water withdrawal, by source and sector, matches reasonably well with reported water withdrawal from AQUASTAT, while water withdrawal by source and sector provide mixed results.

Future work will concentrate on further improving the water withdrawal and water allocation scheme, developing a full dynamic (two-way) coupling with hydrodynamic models, developing 5 km and 1 km resolution (or higher) parameterizations of PCR-GLOBWB 2 using scale-consistent parameterizations (e.g. using MPR;, Samaniego et al., 2017), incorporating a crop growth model and solving the full surface energy balance. Other foreseeable developments are using the model in probabilistic settings and in data-assimilation frameworks.

5. Code and data availability

PCR-GLOBWB 2 is open source and distributed under the terms of the GNU General Public License version 3, or any later version, as published by the Free Software Foundation. The model code is provided through a Github repository: https://github.com/UU-Hydro/PCR-GLOBWB_model (Sutanudjaja et al., 2017a, https://doi.org/10.5281/zenodo.595656). This keeps users and developers immediately aware of any new revisions. Also, it allows developers to easily collaborate, as they can download a new version, make changes, and suggest and upload the newest revisions. The configuration ini-files for the global 30 arc-minutes and 5-arc-minute models and the associated model parameters and input files are provided on https://doi.org/10.5281/zenodo.1045338 (Sutanudjaja et al., 2017b). Development and maintenance of the official version (main branch) of PCR-GLOBWB 2 is conducted at the Department of Physical Geography, Utrecht University. Yet, contributions from external parties are welcome and encouraged. For news on latest developments and papers published based on PCR-GLOBWB 2 we refer to http://www.globalhydrology.nl and for the underlying PCRaster-Python code to http://pcraster.geo.uu.nl.

Acknowledgements

We thank Utrecht University and various grants and projects that directly or indirectly contributed to the development of PCR-GLOBWB 2. The authors are very grateful to all the contributors (as acknowledged in the references) who provided the data sets used in this study. We acknowledge the Netherlands Organisation for Scientific Research (NWO) for the grant that enabled us to use the national super computer Cartesius with the help of SURFsara Amsterdam.

Appendix

Table A1 - List (non-exhaustive) of state and flux variables defined in PCR-GLOBWB

Description	Symbol	Unit
Interception storage	S_{int}	m
Snow cover/storage in water equivalent thickness (excluding liquid part S_{slq})	S_{swe}	m
Liquid/melt water storage in the snow pack	S_{slq}	m
Upper and lower soil storages	S_1 and S_2	m
Surface water storage (lakes, reservoirs, rivers and inundated water)	S_{wat}	m
groundwater storage (renewable part)	S_3	m
fossil groundwater storage (non-renewable)	S_{nrw}	m
total groundwater storage = $S_3 + S_{nrw}$	S_{gwt}	m
total water storage thickness = $S_{int} + S_{swe} + S_{slq} + S_1 + S_2 + S_{gwt}$	TWS	m
potential evaporation	E_{pot}	$m.day^{-1}$
evaporation flux from the intercepted precipitation	E_{int}	$m.day^{-1}$
evaporation from melt water stored in the snow pack	E_{slq}	$m.day^{-1}$
bare soil evaporation	E_{soil}	$m.day^{-1}$
transpiration from the upper and lower soil stores	T_1 and T_2	$m.day^{-1}$
total land evaporation = $E_{pot} + E_{int} + E_{slq} + E_{soil} + T_1 + T_2$	E_{land}	$m.day^{-1}$
surface water evaporation	E_{wat}	$m.day^{-1}$
total evaporation = $E_{land} + E_{wat}$	E_{tot}	$m.day^{-1}$
direct runoff	Q_{dr}	$m.day^{-1}$
interflow, shallow sub-surface flow	Q_{sf}	$m.day^{-1}$
baseflow, groundwater discharge	Q_{bf}	$m.day^{-1}$
specific runoff from land	Q_{loc}	$m.day^{-1}$
local change in surface water storage	Q_{wat}	$m.day^{-1}$
total specific runoff	Q_{tot}	$m.day^{-1}$
routed channel (surface water) discharge	Q_{chn}	$m^3.sec^{-1}$
net fluxes from the upper to lower soil stores	Q_{12}	$m.day^{-1}$
net groundwater recharge, fluxes from the lower soil to groundwater stores	RCH = Q_{23}	$m.day^{-1}$
surface water infiltration to groundwater	Inf	$m.day^{-1}$
desalinated water withdrawal	W_{sal}	$m.day^{-1}$
surface water withdrawal	W_{wat}	$m.day^{-1}$
renewable groundwater withdrawal	W_3	$m.day^{-1}$
non-renewable groundater withdrawal (groundwater depletion)	W_{nrw}	$m.day^{-1}$
total groundwater withdrawal = $W_3 + W_{nrw}$	W_{gwt}	$m.day^{-1}$
water withdrawal allocated for irrigation purpose	A_{irr}	$m.day^{-1}$
water withdrawal allocated for livestock demand/sector	A_{liv}	$m.day^{-1}$
water withdrawal allocated for agricultural sector = $A_{irr} + A_{liv}$	A_{agr}	$m.day^{-1}$
domestic water withdrawal	A_{dom}	$m.day^{-1}$
industrial water withdrawal	A_{ind}	$m.day^{-1}$

Table A2 - List of model inputs and parameters

Description	Symbol	Unit	References/sources
Upper and lower soil store parameters:			FAO (2007) soil map; van Beek and Bierkens (2009)
- Soil thickness	Z_1 and Z_2	m	
- Residual soil moisture content	θ_{r-1} and θ_{r-2}	$m^3.m^{-3}$	
- Soil moisture at saturation	θ_{s-1} and θ_{s-2}	$m^3.m^{-3}$	
- Soil water storage capacity per soil layer: $SC = Z / (\theta_s - \theta_r)$	SC_1 and SC_2	m	
- Soil matric suctions at saturation	ψ_{s-1} and ψ_{s-2}	m	
- Exponent in the soil water retention curve	β_1 and β_2	dimensionless	
- Saturated hydraulic conductivities of upper and lower soil stores	K_1 and K_2	$m.day^{-1}$	
- Total soil water storage capacities = $SC_{upp} + SC_{low}$	W_{max}	m	
Land cover fraction: Land cover areas (including extent of irrigated areas) over cell areas	f_{lcov}	$m^2.m^{-2}$	GLCC v2.0 map (USGS, 1997); Olson (1994a, 1994b); MIRCA2000 dataset (Portmann et al., 2010), FAOSTAT (2012)
Topographical parameters	DEM	m	HydroSHEDS (Lehner et al., 2008); Hydro1k (Verdin and Greenlee, 1996); GTOPO30 (Gesch et al., 1999)
- Cell-average DEM	DEM_{avg}	m	
- Flood plain elevation	DEM_{fpl}	m	
Root fractions per soil layer	Rf_{upp} & Rf_{low}	dimensionless	Canadell et al. (1996); van Beek and Bierkens (2009)
Arno scheme (Todini, 1999; Hagemann and Gates, 2003) exponents defining soil water capacity distribution	β_{arno}	dimensionless	Canadell et al. (1996), Hagemann et al. (1999); Hagemann (2002); van Beek (2008); van Beek and Bierkens (2009)
Ratios of cell-minimum and cell-maximum soil storage to W_{max}	f_{wmin} and f_{wmax}	m	van Beek (2008); van Beek and Bierkens (2009)

Table A2 - List of model inputs and parameters (continued)

Description	Symbol	Unit	References/sources
Parameters related to phenology			Hagemann et al. (1999); Hagemann (2002); van Beek (2008); van Beek and Bierkens (2009)
- Crop coefficient	K_c	dimensionless	
- Interception capacity	$S_{int\text{-}max}$	m	
- Vegetation cover fraction	C_v	$m^2.m^{-2}$	
Groundwater parameters			GLHYMPS map (Gleeson et al., 2014); van Beek (2008); van Beek and Bierkens (2009)
- Aquifer transmissivity	*KD*	$m^2.day^{-1}$	
- Aquifer specific yield	*Sy*	$m^3.m^{-3}$	
- Groundwater recession coefficient	*J*	day^{-1}	
Meteorological forcing			van Beek (2008); CRU (Harris et al., 2014); ERA40 (Uppala et al., 2005); ERA-Interim (Dee et al., 2011)
- Total precipitation	*P*	$m.day^{-1}$	
- Atmospheric air temperature	T_{air}	°C or K	
- Reference potential evaporation and transpiration	$E_{ref,pot}$	$m.day^{-1}$	
Others:			
- Non-irrigation sectoral water demand (i.e. livestock, dometic and industrial)		$m.day^{-1}$	Wada et al (2014)
- Desalinated water		$m.day^{-1}$	Wada et al., (2011a); FAO (2016)
- Lakes and reservoirs			GLWD1 (Lehner and Döll, 2004); GranD (Lehner et al., 2011)

References

Alfieri, L., Burek, P. Dutra, E. Krzeminski, B. Muraro, D. Thielen, J., and Pappenberger F.: GloFAS—Global ensemble streamflow forecasting and flood early warning, Hydrology and Earth System Science, 17, 1161–1175, 2003.

Allen, R.G., Pereira, L.S., Raes, D., and Smith, M.: Crop evaporation: Guidelines for computing crop requirements., UN-FAO, Rome, Italy, 1998.

Argent, R. M.: An overview of model integration for environmental applications–components, frameworks and semantics, Environmental Modelling & Software 19 (3): 219–34, doi:10.1016/S1364-8152(03)00150-6, 2004.

Bates, P.D., Horritt, M. S., and Fewtrell, T.J.: A simple inertial formulation of the shallow water equations for efficient twodimensional flood inundation modelling, Journal of Hydrology, 38, 33–45, 2010.

Bergström, S.: The HBV model, in: Computer Models in Watershed Hydrology, edited by Singh, V. P., Water Resources Publications, Highlands Ranch, CO, 1995.

Beven, K.J. and Cloke, H.L.: Comment on "Hyperresolution global land surface modeling: Meeting a grand challenge for monitoring Earth's terrestrial water" by Eric F. Wood et al., Water Resources Research, 48, 2012.

Bierkens, M.F.P. and van Beek, L.P.H.: Seasonal Predictability of European Discharge: NAO and Hydrological Response Time, Journal of Hydrometeorology 10, 953–968, 2009.

Bierkens, M.F.P., Bell, V.A., Burek, P., Chaney, N., Condon, L.E., David, C.H., de Roo, A., Döll, P., Drost, N., Famiglietti, J. S., Flörke, M., Gochis, D. J., Houser, P., Hut, R., Keune, J., Kollet, S., Maxwell, R. M., Reager, J. T., Samaniego, L., Sudicky, E., Sutanudjaja, E. H., van de Giesen, N., Winsemius, H., and Wood, E. F.: Hyper-resolution global hydrological modelling: what is next? "Everywhere and locally relevant", Hydrological Processes, 29, 310-320, 2014.

Bos, M.G.: Discharge measurement structures, third revised edition, ILRI Wageningen, 1989.

Bosmans, J. H. C., van Beek, L. P. H., Sutanudjaja, E. H., and Bierkens, M. F. P.: Hydrological impacts of global land cover change and human water use, Hydrol. Earth Syst. Sci., 21, 5603-5626, https://doi.org/10.5194/hess-21-5603-2017, 2017. ~~Bosmans, J. H. C., van Beek, L. P. H., Sutanudjaja, E. H., and Bierkens, M. F. P.: Hydrological impacts of global land cover change and human water use, Hydrology and Earth System Science Discussions, https://doi.org/10.5194/hess-21-5603-2017https://doi.org/10.5194/hess-2016-621, 2017~~6.

Campbell, G. S.: A simple method for determining unsaturated conductivity from moisture retention data, Soil Science, 117, 311–314, 1974.

Canadell, J., Jackson, R.B., Ehleringer, J.B. et al: Maximum rooting depth of vegetation types at the global scale, Oecologia, https://doi.org/10.1007/BF00329030, 1996.

Candogan Yossef, N., Winsemius, H. Weerts, A. van Beek, L. P. H, and Bierkens, M.F.P.: Skill of a global seasonal streamflow forecasting system, relative roles of initial conditions and meteorological forcing, Water Resources Research 49, 4687–4699, 2013.

Castronova, A. M. and Goodal, J. L.: A generic approach for developing process-level hydrologic modeling components." Environmental Modelling & Software 25 (7): 819–25. doi:10.1016/j.envsoft.2010.01.003, 2010.

Clapp, R. B. and Hornberger, G. M.: Empirical equations for some soil hydraulic properties, Water Resources Research, 14, 601–604, 1978.

Cohen, S., Kettner, A. J., Syvitski, J. P. M., and Fekete, B. A. M.: WBMsed, a distributed global-scale riverine sediment flux model: Model description and validation, Computers in Geosciences, 53, 80–93, 2013.

Dalin, C., Wada, Y., Kastner, T., and M. J. Puma: Groundwater depletion embedded in international food trade, Nature, 543, 700–704, 2017.

Dankers, R., Arnell, N. W., Clark, D. B., Falloon, P. D., Fekete, B. M., Gosling, S. N., Heinke, J., Kim, H., Masaki, Y., Satoh, Y., Stacke, T., Wada, Y., and Wisser, D.: First look at changes in flood

hazard in the Inter-Sectoral Impact Model Intercomparison Project ensemble, Proceedings of the National Academy of Sciences, 2013.
De Graaf, I. E. M., van Beek, L. P. H., Wada, Y., and Bierkens, M. F. P.: Dynamic attribution of global water demand to surface water and groundwater resources: Effects of abstractions and return flows on river discharges, Advances in Water Resources 64, 21–33, 2014.
De Graaf, I. E. M., Sutanudjaja, E. H., Van Beek, L. P. H., and Bierkens, M. F. P.: A high-resolution global-scale groundwater model. Hydrology and Earth System Sciences, 19, 823-837, 2015.
De Graaf, I. E., van Beek, L.P.H., Gleeson, T., Moosdorf, N., Schmitz, O., Sutanudjaja, E. H., and Bierkens, M. F. P.: A global-scale two-layer transient groundwater model: Development and application to groundwater depletion. Advances in Water Resources, 102, 53-67, 2017.
Dee, D. P., Uppala, S. M., Simmons, A. J., Berrisford, P., Poli, P., Kobayashi, S., Andrae, U., Balmaseda, M. a., Balsamo, G., Bauer, P., Bechtold, P., Beljaars, a. C. M., van de Berg, L., Bidlot, J., Bormann, N., Delsol, C., Dragani, R., Fuentes, M., Geer, a. J., Haimberger, L., Healy, S. B., Hersbach, H., Hólm, E. V., Isaksen, L., Kå llberg, P., Köhler, M., Matricardi, M., McNally, a. P., Monge-Sanz, B. M., Morcrette, J.-J., Park, B.-K., Peubey, C., de Rosnay, P., Tavolato, C., Thépaut, J.-N., and Vitart, F.: The ERA-Interim reanalysis: configuration and performance of the data assimilation system, Quarterly Journal of the Royal Meteorological Society, 137, 553–597, 2011.
Dermody, B. J., van Beek, L. P. H., Meeks, E., Klein Goldewijk, K., Scheidel, W., van der Velde, Y., Bierkens, M. F. P., Wassen, M. J., and Dekker, S. C.: A virtual water network of the Roman world, Hydrology and Earth System Sciences, 18, 5025–5040, http://dx.doi.org/10.5194/hess-18-5025-2014, 2014.
Döll, P. and Siebert, S.: Global modeling of irrigation water requirements, Water Resources Research, 38, 8–1 – 8–10, 2002.
Döll, P., Kaspar, F., and Lehner, B.: A global hydrological model for deriving water availability indicators: model tuning and validation, Journal of Hydrology, 270, 105–134, 2003.
Döll, P., Hoffmann-Dobrev, H., Portmann, F. T., Siebert, S., Eicker, A., Rodell, M., Strassberg, G., and Scanlon, B. R.: Impact of water withdrawals from groundwater and surface water on continental water storage variations, Journal of Geodynamics, 59–60, 143–156, 2012.
Döll, P., Muller Schmied, H., Schuh, Portmann, F. T. and Eicker, A.: Global-scale assessment of groundwater depletion and related groundwater abstractions: Combining hydrological modeling with information from well observations and GRACE satellites, Water Resources Research, 50, 2014.
Doorenbos, J. and Pruitt, W. O.: Crop water requirements, Irrig. Drain. Pap. 24, FAO, Rome, 1977.
Elliott, J., Deryng, D., Müller, C., Frieler, K., Konzmann, M., Gerten, D., Glotter, M., Flörke, M., Wada, Y., Best, N., Eisner, S., Fekete, B. M., Folberth, C., Foster, I., Gosling, S. N., Haddeland, I., Khabarov, N., Ludwig, F., Masaki, Y., Olin, S., Rosenzweig, C., Ruane, A. C., Satoh, Y., Schmid, E., Stacke, T., Tang, Q., and Wisser, D.: Constraints and potentials of future irrigation water availability on agricultural production under climate change, Proceedings of the National Academy of Sciences, 111, 3239–3244, 2013.
Erkens, G. and Sutanudjaja, E. H.: Towards a global land subsidence map, Proc. IAHS, 372, 83-87, https://doi.org/10.5194/piahs-372-83-2015, 2015.
Fekete, B. M. B., Vörösmarty, C. J. C., and Grabs, W.: High-resolution fields of global runoff combining observed river discharge and simulated water balances, Global Biogeochemical Cycles, 16, 10–15, 2002.
Food and Agriculture Organization of the United Nations (FAO): Digital Soil Map of the World, Version 3.6. FAO, Rome, Italy, 2007.
Food and Agriculture Organization of the United Nations (FAO): FAOSTAT statistics database, http://www.fao.org/faostat/en/#home, 2012.
Food and Agriculture Organization of the United Nations (FAO): AQUASTAT database of water-related data. Accessed on [2017-09-15] at: http://www.fao.org/nr/water/aquastat/main/index.stm, 2016.
Gesch, D.B., Verdin, K.L., and Greenlee, S.K.: New Land Surface Digital Elevation Model Covers the Earth: Eos, Transactions, American Geophysical Union, v. 80, no. 6, p. 69–70, 1999.
Gleeson, T., Wada, Y., Bierkens, M. F. P., and van Beek, L. P. H.: Water balance of global aquifers revealed by groundwater footprint, Nature, 488, 197–200, 2012.

Gleeson, T., N. Moosdorf, J. Hartmann, and L. P. H. van Beek: A glimpse beneath earth's surface: GLobal HYdrogeology MaPS (GLHYMPS) of permeability and porosity, Geophys. Res. Lett., 41, 3891–3898, doi:10.1002/2014GL059856, 2014.

Global Soil Data Task: Global Soil Data Products CD-ROM (IGBP-DIS), 2000.

Gosling, S. N. and Arnell, N.W.: Simulating current global river runoff with a global hydrological model: model revisions, validation, and sensitivity analysis, Hydrological Processes, 25, 1129–1145, 2011.

Gupta, H.V., Kling, H., Yilmaz, K.K., and Martinez, G.F.: Decomposition of the mean squared error and NSE performance criteria: Implications for improving hydrological modelling. Journal of Hydrology,377, 80-91, 2009.

Haddeland, I., Heinke, J., Biemans, H., Eisner, S., Flörke, M., Hanasaki, N., Konzmann, M., Ludwig, F., Masaki, Y., Schewe, J., Stacke, T., Tessler, Z. D., Wada, Y., and Wisser, D.: Global water resources affected by human interventions and climate change, Proceedings of the National Academy of Sciences, 111, 3251–3256, ~~2013~~2014.

Hagemann, S., Botzet, M., Dümenil, L., and Machenhauer, B.: Derivation of Global GCM Boundary Conditions from 1 Km Land Use Satellite Data, Max-Planck-Institut für Meteorologie, Hamburg, Germany, 1999.

Hagemann, S.: An improved land surface parameter dataset for global and regional climate models, Max- Planck-Institut für Meteorologie, Hamburg, Germany, https://www.mpimet.mpg.de/fileadmin/publikationen/Reports/max_scirep_336.pdf, 2002.

Hagemann, S. and Gates, L.D.: Improving a subgrid runoff parameterization scheme for climate models by the use of high resolution data derived from satellite observations, Climate Dynamics, 21, 349–359, 2003.

Hagemann, S., Botzet, M., Dümenil, L., and Machenhauer, B.: Derivation of Global GCM Boundary Conditions from 1 Km Land Use Satellite Data, Max-Planck-Institut für Meteorologie, Hamburg, Germany, 1999.

Hamon, W.: Computation of Direct Runoff Amounts from Storm Rainfall, IAHS Publ., 63, 52–62, 1963.

Hanasaki, N., Kanae, S., Oki, T., Masuda, K., Motoya, K., Shirakawa, N., Shen, Y., and Tanaka, K.: An integrated model for the assessment of global water resources - Part 1: Model description and input meteorological forcing, Hydrology and Earth System Science, 12, 1007–1025, 2008.

Hanasaki, N., S. Kanae, T. Oki, K. Masuda, K. Motoya, N. Shirakawa, Y. Shen, and K. Tanaka (2008b), An integrated model for the assessment of global water resources - Part 2: Applications and assessments, Hydrology and Earth System Science, 12, 1027–103.

Hanasaki, N., Yoshikawa, S., Pokhrel, Y.and Kanae, S. A global hydrological simulation to specify the sources of water used by humans Hydrology and Earth System Science, 22, 789-817, 2018

Harbaugh, A.W., Banta, E.R., Hill, M.C., and McDonald, M.G., 2000, MODFLOW-2000, the U.S. Geological Survey modular ground-water model -- User guide to modularization concepts and the Ground-Water Flow Process: U.S. Geological Survey Open-File Report 00-92, 121 p

Harris, I., Jones, P., Osborn, T., and Lister, D.: Updated high-resolution grids of monthly climatic observations - the CRU TS3.10 Dataset, International Journal of Climatology, 34, 623–642, 2014.

Hirabayashi Y., M. Roobavannan, K. Sujan, K. Lisako, Y. Dai, W. Satoshi, K. Hyungjun, and K. Shinjiro (2013), Global flood risk under climate change, Nature Climate Change, 3, 816–821.

Hoch, J.M., Haag, Arjen, van Dam, Arthur, Winsemius, Hessel, van Beek, L.P.H. & Bierkens, M.F.P.: Assessing the impact of hydrodynamics on large-scale flood wave propagation - a case study for the Amazon Basin, Hydrology and Earth System Science, 21, 117-132, 2017a.

Hoch, J.M., Neal, J.C., Baart, F. van Beek, L.P.H., Winsemius, H.C., Bates, P.D., and Bierkens, M.F.P.: GLOFRIM v1.0 – A globally applicable computational framework for integrated hydrological-hydrodynamic modelling. Geoscientific Model Development, 10, 3913-3929, 2017b.

Karssenberg, D., de Jong K., and van der Kwast, J.: Modelling landscape dynamics with Python, International Journal of Geographical Information Science, 21, 483-495, 2007.

Karssenberg, D., Schmitz, O., Salamon, P., de Jong, K., and Bierkens, M. F. P.: A software framework for construction of process-based stochastic spatio-temporal models and data assimilation, Environmental Modelling & Software, 25, 489–502, 2010.

Kauffeldt, A., Wetterhall, F., Pappenberger, F., Salamon, P., and Thielen, J.: Technical review of large-scale hydrological models for implementation in operational flood forecasting schemes on continental level. Environmental Modelling and Software, 75, 68–76, 2016.
Kernkamp, H.W.J., van Dam, A., Stelling, G.S. and de Goede, E.D.: Efficient scheme for the shallow water equations on unstructured grids with application to the Continental Shelf, Ocean Dynamics. 61, 1175–1188, 2011.
Konar, M., Hussein, Z., Hanasaki, N., Mauzerall, D. L., and Rodriguez-Iturbe, I.: Virtual water trade flows and savings under climate change, Hydrology and Earth System Science, 17, 3219–3234, 2013.
Konikow, L. F.: Contribution of global groundwater depletion since 1900 to sea-level rise, Geophysical Research Letters 38, L17401, 1-5, 2011.
Kraijenhoff van de Leur, D.A.: A study of non-steady ground-water flow with special reference to the reservoir-coefficient, De Ingenieur 19, 87-94, 1958.
Lehner, B. and Döll, P.: Development and validation of a global database of lakes, reservoirs and wetlands, Journal of Hydrology 296, 1–22, 2004.
Lehner, B., Verdin, K., and Jarvis, A.: New global hydrography derived from spaceborne elevation data, Eos (Washington. DC)., 89, DOI: 10.1029/2008EO100001, 2008.
Lehner, B., Reidy Liermann, C., Revenga, C., Vörösmarty, C., Fekete, B., Crouzet, P., Döll, P., Endejan, M., Frenken, K., Magome, J., Nilsson, C., Robertson, J., Rödel, R., Sindorf, N., and Wisser, D.: High- resolution mapping of the world's reservoirs and dams for sustainable river-flow management. Frontiers in Ecology and the Environment, 9 494–502, 2011.
Liang, X., Lettenmaier, D. P., Wood, E. F., and Burges, S. J.: A simple hydrologically based model of land surface water and energy fluxes for general circulation models, Journal of Geophysical Research, 99, 14415–14428, 1994.
Loveland, T. R., Reed, B. C., and Brown, J. F.: Development of a global land cover characteristics database and IGBP DISCover from 1 km AVHRR data, International Journal of Remote Sensing, 21, 1303–1330, 2000.
McDonald, R. I., Weber, K., Padowski, J., Flörke, M., Schneider, C., Green, P. A., Gleeson, T. Eckman, S. Lehner, B. Balk, D., Boucher, T. Grill, G. and Montgomery, M.: Water on an urban planet: Urbanization and the reach of urban water infrastructure. Global Environmental Change, 27, 96-105, 2011.
Murray, F.: On the computation of saturation vapor pressure, IAHS Publ., 6, 203–204, 1967.
New, M., Lister, D., Hulme, M., and Makin, I.: A high-resolution data set of surface climate over global land areas, Climate Research, 21, 1–25, 2002.
Nijssen, B., O'Donnell, G. M., Lettenmaier, D. P., Lohmann, D., and Wood, E. F.: Predicting the Discharge of Global Rivers, Journal of Climate, 14, 3307–3323, 2001.
Oki, T. and Kanae, S.: Global hydrological cycles and world water resources, Science, 313, 1068–1072, 2006.
Olson, J. S.: Global ecosystem framework-definitions, Tech. rep., USGS EROS Data Center Internal Report, Sioux Falls, SD, 1994a.
Olson, J. S.: Global ecosystem framework-translation strategy, Tech. rep., USGS EROS Data Center Internal Report, Sioux Falls, SD, 1994b.
Pappenberger, F., Dutra, E., Wetterhall, F., and Cloke, H.L.: Deriving global flood hazard maps of fluvial floods through a physical model cascade, Hydrology and Earth System Science, 16, 4143–4156, 2012.
Pokhrel, Y. N., Hanasaki, N., Yeh, P. J., Yamada, T. J., Kanae, S., and Oki, T.: Model estimates of sea-level change due to anthropogenic impacts on terrestrial water storage. Nature Geoscience, 5, 389-392, 2012.
Pokhrel, Y. N., Koirala, S. Yeh, P. J.-F., Hanasaki, N., Longuevergne, L., Kanae, S., and Oki, T.: Incorporation of groundwater pumping in a global Land Surface Model with the representation of human impacts, Water Resources Research, 51, 2015.
Portmann, F. T., Siebert, S., and Döll, P.: MIRCA2000-Global monthly irrigated and rainfed crop areas around the year 2000: A new high-resolution data set for agricultural and hydrological modeling, Global Biogeochemical Cycles, GB1011, 1-24, 2010.

Prudhomme, C., Giuntoli, I., Robinson, E. L., Clark, D. B., Arnell, N. W., Dankers, R., Fekete, B. M., Franssen, W., Gerten, D., Gosling, S. N., Hagemann, S., Hannah, D. M., Kim, H., Masaki, Y., Satoh, Y., Stacke, T., Wada, Y., and Wisser, D.: Hydrological droughts in the 21st century, hotspots and uncertainties from a global multimodel ensemble experiment, Proceedings of the National Academy of Sciences, 111, 3262–3267, 2013.

Rodell, M., ; Beaudoing, H. K., ; L'Ecuyer, T. S., ; Olson, W. S., ; Famiglietti, J. S., ; Houser, P. R., ; Adler, R., ; Bosilovich, M. G., ; Clayson, C. A., ; Chambers, D., ; Clark, E., ; Fetzer, E. J., ; Gao, X., ; Gu, G., ; Hilburn, K., ; Huffman, G. J., ; Lettenmaier, D. P., ; Liu, W. T., ; Robertson, F. R., ; Schlosser, C. A., ; Sheffield, J., ; Wood, E. F.: The Observed State of the Water Cycle in the Early Twenty-First Century. Journal of Climate, 28, 8289-8318, 2012.

Rohwer J, Gerten D, Lucht W. Development of functional irrigation types for improved global crop modelling. PIK Report 104, 2007.

Rost, S., Gerten, D., and Heyder, U.: Human alterations of the terrestrial water cycle through land management, Advances in Geosciences, 18, 43–50, 2008.

Samaniego, L. Kumar, R., Thober, S., Rakovec, O., Zink, M., Wanders, N., Eisner, S., Müller Schmied, H., Sutanudjaja, E.H., Warrach-Sagi K., and Attinger, S.: Toward seamless hydrologic predictions across spatial scales, Hydrology and Earth System Science, 21, 4323-4346, 2017.

Savenije, H. H. G.: The importance of interception and why we should delete the term evaporation from our vocabulary, Hydrological Processes, 18, 1507–1511, 2004.

Schewe, J., Heinke, J., Gerten, D., Haddeland, I., Arnell, N. W., Clark, D. B., Dankers, R., Eisner, S., Fekete, B. M., Colón-González, F. J., Gosling, S. N., Kim, H., Liu, X., Masaki, Y., Portmann, F. T., Satoh, Y., Stacke, T., Tang, Q., Wada, Y., Wisser, D., Albrecht, T., Frieler, K., Piontek, F., Warszawski, L., and Kabat, P.: Multimodel assessment of water scarcity under climate change, Proceedings of the National Academy of Sciences, 111, 3245–3250, 20132014.

Sheffield, J., Wood, E. F., and Munoz-Arriola, F.: Long-Term Regional Estimates of Evaporation for Mexico Based on Downscaled ISCCP Data, Journal of Hydrometeoroly, 11, 253–275, 2010.

Siebert, S., Döll, P., Hoogeveen, J., Faures, J.-M., Frenken, K., and Feick, S.: Development and validation of the global map of irrigation areas, Hydrology and Earth System Science, 9, 535–547, 2005.

Siebert, S. and Döll, P.: Quantifying blue and green virtual water contents in global crop production as well as potential production losses without irrigation, Journal of Hydrology, 384, 198–217, 2010.

Siebert, S., Burke, J., Faures, J. M., Frenken, K., Hoogeveen, J., Döll, P., and Portmann, F. T.: Groundwater use for irrigation–a global inventory. Hydrology and Earth System Sciences, 14(10), 1863-1880, 2010.

Siebert, S., Henrich, V., Frenken, K., Burke, J.: Update of the Global Map of Irrigation Areas to version 5. Project report, 178 p., 2013.

Sloan, P.G. and I.D. Moore: Modeling subsurface stormflow on steeply sloping forested watersheds, Water Resources Research 20, 1815–1822, 1984.

Sperna Weiland, F. C., van Beek, L. P. H., Kwadijk, J. C. J., and Bierkens, M. F. P.: Global patterns of change in discharge regimes for 2100, Hydrology and Earth System Science, 16, 1047–1062, 2012.

Sterling, S. M., Ducharne, A., and Polcher, J.: The impact of global land-cover change on the terrestrial water cycle, Nature Climate Change, 3, 385–390, 2013.

Sutanudjaja, E. H., van Beek, L. P. H., de Jong, S. M., van Geer, F. C., and Bierkens, M. F. P.: Large-scale groundwater modeling using global datasets: a test case for the Rhine-Meuse basin, Hydrology and Earth System Science, 15, 2913–2935, 2011.

Sutanudjaja, E. H.: The use of soil moisture remote sensing products for large-scale groundwater modeling and assessment, PhD thesis, Utrecht Univ., Netherlands, 2012.

Sutanudjaja, E. H., van Beek, L. P. H., de Jong, S. M., van Geer, F. C., and Bierkens, M. F. P.: Calibrating a large-extent high-resolution coupled groundwater-land surface model using soil moisture and discharge data, Water Resources Research, 50, 687–705, 2014.

Sutanudjaja, E.H., van Beek, Rens, Wanders, Niko, Wada, Yoshihide, Bosmans, Joyce, Drost, Niels, van der Ent, Ruud, de Graaf, Inge, Hoch, Jannis, de Jong, Kor, Karssenberg, Derek, López López, Patricia, Peßenteiner, Stefanie, Schmitz, Oliver, Straatsma, Menno, Vannametee, Ekkamol, Wisser, Dominik and Bierkens, Marc: PCR-GLOBWB_model: PCR-GLOBWB version v2.1.0_beta_1, , doi:10.5281/zenodo.247139, 2017a.

1272 Sutanudjaja, E.H., van Beek, Rens, Wanders, Niko, Wada, Yoshihide, Bosmans, Joyce, Drost, Niels,
1273 van der Ent, Ruud, de Graaf, Inge, Hoch, Jannis, de Jong, Kor, Karssenberg, Derek, López López,
1274 Patricia, Peßenteiner, Stefanie, Schmitz, Oliver, Straatsma, Menno, Vannametee, Ekkamol, Wisser,
1275 Dominik and Bierkens, Marc: PCR-GLOBWB 2 input files version 2017_11_beta_1,
1276 doi:10.5281/zenodo.1045339, 2017b.
1277 The Global Runoff Data Centre (GRDC): The Global Runoff Database and River Discharge Data.
1278 56068 Koblenz, Germany. Data were requested from http://www.bafg.de/GRDC and made available
1279 for us on 17 April 2014, 2014.
1280 Todini, E.: The ARNO rainfall-runoff model, Journal of Hydrology, 175, 339–382, 1996.
1281 Uppala, S.M. et al.: The ERA-40 re-analysis, Quarterly Journal of the Royal Meteorological Society
1282 131, 2961–3012, 2005.
1283 USGS EROS Data Center: HYDRO1k Elevation Derivative Database, LP DAAC:
1284 http://edcdaac.usgs.gov/gtopo30/hydro/, 2006.
1285 Van Beek, L. P. H.: Forcing PCR-GLOBWB with CRU data, Tech. rep., Department of Physical
1286 Geography, Utrecht University, Utrecht, The Netherlands,
1287 http://vanbeek.geo.uu.nl/suppinfo/vanbeek2008.pdf, 2008.
1288 Van Beek, L. P. H. and Bierkens, M. F. P.: The Global Hydrological Model PCR-GLOBWB:
1289 Conceptualization, Parameterization and Verification, Tech. rep., Department of Physical
1290 Geography, Utrecht University, Utrecht, The Netherlands,
1291 http://vanbeek.geo.uu.nl/suppinfo/vanbeekbierkens2009.pdf, 2009.
1292 Van Beek, L. P. H., Wada, Y., and Bierkens, M. F. P.: Global monthly water stress: 1. Water balance
1293 and water availability, Water Resources Research, 47, W07 517, 2011.
1294 Van Beek, L. P. H., Eikelboom, T., van Vliet, M. T. H. and Bierkens, M. F. P.: A physically based
1295 model of global freshwater surface temperature, Water Resources Research, 48, W09530,
1296 doi:10.1029/2012WR011819, 2012.
1297 Van Vliet, M. T. H., Yearsley, J. R. F. Ludwig, Vögele, S, Lettenmaier, D.P. and Kabat, P.:
1298 Vulnerability of US and European electricity supply to climate change, Nature Climate Change, 2,
1299 676–681, 2012.
1300 Verdin, K.L., and Greenlee, S.K.,: Development of continental scale digital elevation models and
1301 extraction of hydrographic features. In: Proceedings, Third International Conference/Workshop on
1302 Integrating GIS and Environmental Modeling, Santa Fe, New Mexico, January 21-26, 1996.
1303 National Center for Geographic Information and Analysis, Santa Barbara, California, 1996.
1304 Vörösmarty, C. J., Leveque, C., and Revenga, C.: Millennium Ecosystem Assessment Volume 1:
1305 Conditions and Trends, chap. 7: Freshwater ecosystems, Island Press, Washington DC, USA, 165–
1306 207, 2005.
1307 Wada, Y., van Beek, L. P. H., van Kempen, C. M., Reckman, J. W. T. M., Vasak, S., and Bierkens, M.
1308 F. P.: Global depletion of groundwater resources, Geophys. Res. Lett., 37, L20 402, 1-5, 2010.
1309 Wada, Y., van Beek, L. P. H., Viviroli, D., Dürr, H. H., Weingartner, R., and Bierkens, M. F. P.: Global
1310 monthly water stress: 2. Water demand and severity of water stress, Water Resources Research, 47,
1311 W07 518, 1-17, 2011a.
1312 Wada, Y., van Beek, L. P. H. and Bierkens, M.F P.: Modelling global water stress of the recent past:
1313 On the relative importance of trends in water demand and climate variability, Hydrology and Earth
1314 System Science, 15, 3785–3808, 2011b.
1315 Wada, Y., van Beek, L. P. H., and Bierkens, M. F. P.: Nonsustainable groundwater sustaining
1316 irrigation: A global assessment, Water Resources Research, 48,1-18, 2012a.
1317 Wada, Y., van Beek, L. P. H., Sperna Weiland, F. C., Chao, B. F., Wu, Y.-H., and Bierkens, M. F. P.:
1318 Past and future contribution of global groundwater depletion to sea-level rise, Geophysical Research
1319 Letters, 39, L09402, 1-6, 2012b.
1320 Wada, Y., van Beek, L.P.H., Wanders N., and Bierkens, M.F.P.: Human water consumption intensifies
1321 hydrological drought worldwide. Environmental Research Letters 8, 034036, 2013.
1322 Wada, Y., Wisser, D., and Bierkens, M. F. P.: Global modeling of withdrawal, allocation and
1323 consumptive use of surface water and groundwater resources, Earth System Dynamics, 5, 15–40,
1324 2014.
1325 Wada, Y., and M. F. P. Bierkens: Sustainability of global water use: past reconstruction and future
1326 projections, Environmental. Research Letters, 9, 104003, 2014.

Wada, Y., de Graaf, I.E.M., and van Beek, L.P.H.: High-resolution modeling of human and climate impacts on global water resources, Journal of Advances in Modeling Earth Systems, 8, 735–763, 2016.
Wanders, N., Wada, Y., and Van Lanen, H. A. J.: Global hydrological droughts in the 21st century under a changing hydrological regime. Earth System Dynamics, 6, 1–15, 2015
Wanders, N. and Wada, Y.: Decadal predictability of river discharge with climate oscillations over the 20th and early 21st century, Geophysical Research Letters, 42, 10689-10695, 2015
Wanders, N. and Wada, Y.: Human and climate impacts on the 21st century hydrological drought. Journal of Hydrology, 526, 208-220, 2016
Ward, P. J., Jongman, B., Sperna-Weiland, F., Bouwman, A., van Beek, L. P. H., Bierkens, M. F. P., Ligtvoet, W., and Winsemius, H.C.: Assessing flood risk at the global scale: Model setup, results, and sensitivity, Environmental Research Letters, 8, 044019, 2013.
Watkins, M. M., Wiese, D. N., Yuan, D.-N., Boening, C. and Landerer, F.W.: Improved methods for observing Earth's time variable mass distribution with GRACE using spherical cap mascons, Journal of Geophysical Research - Solid Earth, 120, 2648–2671, 2015.
Wesseling, C. G., Karssenberg, D., van Deursen, W. P. A., and Burrough, P. A.: Integrating dynamic environmental models in GIS: The development of a Dynamic Modelling language, Transaction in GIS, 1, 40–48, 1996.
Wiese. D.N.: GRACE monthly global water mass grids NETCDF RELEASE 5.0. Ver. 5.0. PO.DAAC, CA, USA. Dataset accessed [2017-09-15] at http://dx.doi.org/10.5067/TEMSC-OCL05, 2015.
Wiese, D. N., Landerer, F. W., and Watkins M. M.: Quantifying and reducing leakage errors in the JPL RL05M GRACE mascon solution, Water Resources Research, 52, 7490–7502, 2016.
Winsemius, H. C., Van Beek, L. P. H., Jongman, B., Ward, P. J., and Bouwman, A.: A framework for global river flood risk assessments, Hydrology and Earth System Science, 17, 1871–1892, 2013.
Winsemius, H. C., Aerts, J. C., van Beek, L. P., Bierkens, M. F.P., Bouwman, A., Jongman, B., Kwadijk, J. C., Ligtvoet, W., Lucas, P. L., van Vuuren, D. P., and Ward, P.J.: Global drivers of future river flood risk, Nature Climate Change, 6, 381–385, 2016.
Wisser, D., Fekete, B. M., Vörösmarty, C. J., and Schumann, A. H.: Reconstructing 20th century global hydrography: a contribution to the Global Terrestrial Network- Hydrology (GTN-H), Hydrology and Earth System Sciences, 14, 1–24, 2010.
Wood, E. F., Roundy, J. K., Troy, T. J., van Beek, L. P. H., Bierkens, M. F. P., Blyth, E., de Roo, A., Döll, P., Ek, M., Famiglietti, J., Gochis, D., van de Giesen, N., Houser, P., Jaffé, P. R., Kollet, S., Lehner, B., Lettenmaier, D. P., Peters-Lidard, C., Sivapalan, M., Sheffield, J., Wade, A., and Whitehead, P.: Hyperresolution global land surface modeling: Meeting a grand challenge for monitoring Earth's terrestrial water, Water Resources Research, 47, W05 301, 1-10, 2011.